Could narrow marine embayments prevent sea-glacier invasion, and protect photosynthetic life during a Snowball Earth?

Adam J. Campbell

A dissertation submitted in partial fulfillment of the
requirements for the degree of

Doctor of Philosophy

University of Washington

2015

Reading Committee:

Edwin D. Waddington, Chair

Stephen G. Warren, Chair

Dale P. Winebrenner

Program Authorized to Offer Degree:
Earth and Space Sciences

University of Washington

Abstract

Could narrow marine embayments prevent sea-glacier invasion, and protect photosynthetic life during a Snowball Earth?

Adam J. Campbell

Co-Chairs of the Supervisory Committee:
Professor Edwin D. Waddington
Earth and Space Sciences

Professor Stephen G. Warren
Astrobiology Program, Atmospheric Sciences, Earth and Space Sciences

During the Snowball Earth events of the Neoproterozoic, the Earth's oceans may have been completely covered in ice. This ice would have been thick enough to prohibit the transmission of light to the liquid water underneath the entirely frozen surface of the ocean. However, photosynthetic eukaryotes are thought to have survived during these events. This is the first work to throughly attempt to reconcile how photosynthetic eukaryotes survived on a planet with a completely frozen ocean surface. Narrow marine embayments like the modern-day Red Sea, would restrict the inflow of sea glaciers. These embayments, if located in regions of net sublimation, would restrict sea-glacier invasion and could provide refuge for these organisms at the end of their channels. This work demonstrates that under a set of climate conditions and channel geometries, narrow marine embayments allow for incomplete sea-glacier invasion, a necessary condition for marine embayments to provide refugia

TABLE OF CONTENTS

Page

List of Figures ii

Acknowledgements iii

Dedication iv

Chapter 1: Motivation 1

Chapter 2: Survival of life on the Snowball Earth of the Neoproterozoic 2
2.1 Problem statement 3

Chapter 3: Refugium for surface life on Snowball Earth in a nearly-enclosed sea? A first simple model for sea-glacier invasion 4

Chapter 4: Refugium for surface life on Snowball Earth in a nearly enclosed sea? A numerical solution for sea-glacier invasion through a narrow strait . 19

Chapter 5: Can promontories restrict sea-glacier penetration into marine embayments during Snowball Earth events? 33

Chapter 6: Conclusions drawn from this work 52

Chapter 7: Thoughts and ideas for further research 53
7.1 Climate of inland seas 53
7.2 Grounding of sea glaciers 55
7.3 Land glaciers 57
7.4 Nutrient supply 60

Bibliography 61

LIST OF FIGURES

Figure Number Page

7.1 Cartoons of inland sea climate modeling 55
7.2 Climate of a Snowball Continent 59

ACKNOWLEDGMENTS

I would like to thank the members of my committee, Cecilia Bitz, Edwin Waddington, Stephen Warren and Dale Winebrenner. LuAnne Thompson served as my graduate student representative.

Christina Hulbe has been a mentor to me for many years. I'm excited to continue working with her.

I'd like to especially thank Olga Sergienko for her extensive help with getting my numerical ice flow model working.

I'm had many great conversations about Snowball Earth with many bright and talented individuals. This list isn't exhaustive, but I'd like to thank: Regina Carns, Michelle Koutnik, Gerard, Roe, Charlie Raymond, Lizzy Stefurak, Brian Rose, Huiming Bao, David Catling, Juliet Crider, Francis MacDonald, Paul Hoffman, Dorian Abbot, Heidi Houston, Darrel Cowan, Jodi Bourgeois, Charlotte Schreiber, Ray Pierrehumbert, Mark Skidmore, Bonnie Light, and John Booker.

The glaciology group here at the University of Washington has been very helpful and I've enjoyed many lively conversations at glaciology lunch over the past years.

I'd like to thank T.J. Fudge for motivation, modeling help, useful discussions, and most importantly, inspiring me to make my, now famous, Green Algae Man.

I would to thank Jon Bapst, Elena Amador and Matt Smith for manuscript editing and figure making.

The graduate students in the Earth and Space Sciences department at the University of Washington have been like a family to me. Their support has been tremendous.

My girlfriend Janet encouraged me in this process when I needed it the most.

Last but not least, I'd like to thank my family for always supporting me to follow my dreams and ride the crazy wave of life to where it takes me.

DEDICATION

I dedicate this work to my late brother Jason H. Campbell.
He was not with us long enough, but is still remembered and loved.

"Ring the bells that still can ring
forget your perfect offering
theres a crack in everything
thats how the light gets in"
-Leonard Cohen

Chapter 1

MOTIVATION

I have spent the last few years considering the incredible Snowball Earth events of the Neoproterozoic. I have found it fascinating to consider a vision of time when the entire Earth was locked in a shell of ice and snow. However, I have learned that this simple vision may not describe exactly how that Earth looked. While researching the Snowball Earth events I've considered many questions:

How did the entire planet become this frozen wasteland? How did the planet recover into its present warm and lush state? If our planet's climate could have changed so dramatically, did other planets in our solar system look different during their distant pasts? If life could survive on a Snowball Earth, could life survive (or thrive) on other frozen planets? Can we learn anything about our Earth's present climate change by examining our planet's extreme Snowball climate?

These questions have motivated me during my studies here at the University of Washington. I am unable to answer all these questions. Here I focus on one question. Where did life survive on such a hostile place? I have made a considerable stride toward answering this question and hopefully provided insight into the vision of the Snowball Earth events.

Chapter 2

SURVIVAL OF LIFE ON THE SNOWBALL EARTH OF THE NEOPROTEROZOIC

There is evidence that the Earth's ocean surface may have completely frozen over during the Neoproterozoic [Hoffman and Schrag, 2002]. The oceans during Marinoan and Sturtian glaciations, commonly referred to as the Snowball Earth events, are thought have been covered by sea glaciers, ice hundreds of meters thick and deforming under their own weight. Dropstones from these glaciation events have been discovered in many locations with near-equatorial paleo-latitudes, which along with other evidence, indicates frozen conditions on the tropical ocean during these periods. Energy balance models demonstrate that a climate allowing some frozen ocean at the equator is likely completely frozen over [Sellers, 1969, Budyko, 1969]. These two ideas were merged by Kirschvink [1992] into the Snowball Earth hypothesis.

Photosynthetic eukaryotic algae existed immediately prior to and after these events [Knoll, 1992, Macdonald et al., 2010] so they are presumed to have survived during Snowball Earth. These algae require both liquid water and sunlight. It is not immediately clear where such conditions could co-exist on a planet with an entirely frozen ocean surface. This apparent discrepancy has inspired searches for stable climate states capable of maintaining open ocean conditions near the equator [Hyde et al., 2000, Liu and Peltier, 2010, Pollard and Kasting, 2005, Abbot et al., 2011]. In these scenarios, mountain glaciers may have reached the oceans near the equator, while the ocean surface maintains large areas of open ocean near the equator. Hoffman and Schrag [2000] suggested a potential refugium for life for an ocean without an open water zone, small pools of open water that could be maintained above geo-thermal hotspots on coastlines of volcanic islands. Here I explore another possible refugium, narrow marine embayments, which are possible with an ocean without an open water zone, and with a much larger area than pools over geo-thermal hotspots. This work

is the first attempt to rigorously demonstrate the viability of this class of refugium for photosynthetic life during the Snowball Earth events.

Marine embayments are an attractive class of refugia because of their potential size, number and lifetime. A narrow arm of the ocean can be formed by continental rifting, such as the modern Red Sea. The global sea glacier would invade such an arm; however if the arm was located in a zone of net sublimation, the sea glacier might entirely sublimate away before penetrating the entire channel. If the sea glacier was incapable of fully penetrating into a marine embayment, the remaining un-invaded embayment may act as a refugium. The embayment would have achieved one condition necessary for being a refugium.

2.1 Problem statement

In order for a marine embayment to provide a refugium for photosynthetic life during the Snowball Earth events, it must restrict sea-glacier invasion. Here, I test if, and under what climate and geometric conditions, a marine embayment can restrict invasion of a sea glacier. In the first paper (Chapter 3), I use a simple analytical model to determine what climate conditions restrict sea-glacier invasion. In the second paper (Chapter 4), a more sophisticated model is used to explore the effect of narrow entrances on sea-glacier penetration, and in the third paper (Chapter 5) a model is used to examine the impact of obstructions in the channel.

Chapter 3

REFUGIUM FOR SURFACE LIFE ON SNOWBALL EARTH IN A NEARLY-ENCLOSED SEA? A FIRST SIMPLE MODEL FOR SEA-GLACIER INVASION

Originally published in Geophysical Research Letters

Adam J. Campbell, Edwin D. Waddington, and Stephen G. Warren. Refugium for surface life on Snowball Earth in a nearly-enclosed sea? A first simple model for sea-glacier invasion. *Geophysical Research Letters*, 38(19):1 5, October 2011. ISSN 0094-8276. doi: 10.1029/2011GL048846. URL http://www.agu.org/pubs/crossref/2011/2011GL048846.shtml.

This first paper was aimed at determining whether inland seas could have been refugia for photosynthetic life during the Snowball Earth events of the Neoproterozoic. A first step at answering that question is to determine whether sea glaciers would fully penetrate into inland seas or would sublimate away before reaching the end. To answer this question, I developed a 1-D force balance model using a velocity solution from Nye [1965] where he considered a glacier of infinite thickness whose flow is resisted by two parallel sidewalls. This paper demonstrates Nye's model is equivalent to a floating sea glacier flowing into a parallel walled embayment. We were then able to calculate the penetration length of a sea glacier invading into a channel with two parallel side walls. Penetration distance is compared to the length a modern analogue for a parallel sided channel. We discovered that for a range of climate conditions, a sea glacier would incompletely penetrate a channel.

In order for an inland sea to have provided a refugium for photosynthetic life, it must have remained free of sea-glacier invasion for the duration of the Snowball Earth event. As the planet gradually warms through the duration of the Snowball Earth event, two things happen: ice warms, allow it to flow with less resistance, and sublimation will increase. These two effects compete at controlling the length of the invading sea glacier as the planet warms. We discover the sum of these two effects is to diminish sea-glacier penetration as

the planet warms.

This work has provided a basis for comparison and an expansion point for other works that have since been published. This paper used a simplified 1-D model for ice flow and was limited to channels with parallel-sided walls. We later considered the effect of a narrow entrance in Chapter 4 using a 2-D ice flow model. A later independent study showed close agreement with the penetration length of sea glaciers moving through continental constrictions [Tziperman et al., 2012]. Abbot et al. [2013] expanded our work here to consider the change in upstream ice thickness supplied to inland seas as the planet warms. They added robustness to our conclusion that sea-glacier penetration is diminished as the the planet warms.

For this work, I developed the solution for the ice-flow model and calculated the change in ice penetration during a warming Snowball Earth. E. D. Waddington calculated the effective ice softness in a manner that ensures the horizontal strain rate is uniform in the deforming ice, he also verified all the ice flow calculations. S. G. Warren helped provide much of the background context of Snowball Earth.

There are a few final notes on the works presented here in this chapter. There were 2 errors in this publication; they have been corrected in Appendix A of Campbell et al. [2014], presented here in Chapter 4. These errors do not affect of the conclusions originally made. The publication is reproduced here in its original, uncorrected form. Do not be alarmed by the 'DRAFT' label on the Supplemental presented material here, that is the official version that *Geophysical Research Letters* has chosen to publish.

GEOPHYSICAL RESEARCH LETTERS, VOL. 38, L19502, doi:10.1029/2011GL048846, 2011

Refugium for surface life on Snowball Earth in a nearly-enclosed sea? A first simple model for sea-glacier invasion

Adam J. Campbell,[1] Edwin D. Waddington,[1] and Stephen G. Warren[1,2]

Received 8 July 2011; revised 22 August 2011; accepted 24 August 2011; published 8 October 2011.

[1] The existence of photosynthetic eukaryotic algae during the so-called Snowball Earth events presents a conundrum. If thick ice covered the oceans, where could such life persist? Here we explore the possibility that photosynthetic life persisted at the end of long narrow seas, analogous to the modern-day Red Sea. In this first analytical model, we test the ability of the global sea glacier to penetrate a Red Sea analogue under climatic conditions appropriate during a Snowball Earth event. We find the Red Sea is long enough to provide a refugium only if certain ranges of climatic conditions are met. These ranges would likely expand if the restrictive effect of a narrow entrance strait is also considered. **Citation:** Campbell, A. J., E. D. Waddington, and S. G. Warren (2011), Refugium for surface life on Snowball Earth in a nearly-enclosed sea? A first simple model for sea-glacier invasion, *Geophys. Res. Lett.*, *38*, L19502, doi:10.1029/2011GL048846.

1. Introduction

[2] During the low-latitude glaciation of the Neoproterozoic, 600–800 Ma [*Evans*, 2000; *Harland*, 1964], the upper ocean may have become almost completely covered with thick ice, commonly known as Snowball Earth events [*Kirschvink*, 1992; *Hoffman et al.*, 1998; *Warren et al.*, 2002; *Pierrehumbert et al.*, 2011]. Photosynthetic eukaryotic algae did survive these events [*Knoll*, 1992; *Macdonald et al.*, 2010], indicating that liquid water was maintained at some locations at or near the ocean surface. In the face of evidence for global ocean ice cover, how did open water and life persist? With an equilibrium ice thickness (set by geothermal flux) reaching hundreds of meters, but thicker at high latitude than at low latitude, the floating ice would flow equatorward as a "sea glacier" [*Goodman and Pierrehumbert*, 2003], threatening to invade any unprotected areas of open water. Small pools of open water could be maintained above geothermal hotspots on coastlines of volcanic islands [*Hoffman and Schrag*, 2000], where the water is shallow enough that the geothermal heat is not diffused laterally and that the sea glacier becomes grounded and slowed by friction with the sea floor.

[3] Here we investigate a possible class of refugia, isolated refuges for life, that could be much larger and also longer-lasting. A long narrow arm of a sea, for example as formed by continental rifting such as the modern Red Sea, located at low latitude and surrounded by desert land, would be invaded by a tongue of the global sea glacier, but this tongue would be impeded by friction with the sidewalls and thinned by sublimation, so that its thickness would diminish to zero before reaching the end of the sea, if the sea is long enough. This possibility was mentioned by *Warren et al.* [2002] and considered likely by *Pollard and Kasting* [2005, 2006]. The low-albedo (non-glaciated) land surrounding the bay at the inland end of the narrow sea might keep the bay warm enough to allow open water, even while the rest of the ocean was kept cold by its high albedo. In a GCM simulation of Snowball Earth, a rectangular continent centered on the equator did have higher average temperatures than the equatorial ocean, particularly at the eastern end of the continent [*Abbot and Pierrehumbert*, 2010].

[4] In this paper we investigate only one aspect of this problem, namely the criterion for preventing the sea glacier from reaching the inland end of the sea. This is a necessary, but not sufficient, condition for the existence of a refugium. If the climate at the end of a narrow sea is too cold, the sea will fill with thick ice grown locally, even without any inflow from the global sea glacier. But even if the climate is warm enough to sustain open water or thin ice in the absence of ice flow, sea-glacier invasion could destroy the refugium. To isolate and explore this latter threat, we consider temperature regimes that are otherwise favorable to a refugium. In this first exercise, we further simplify the problem by considering only a sea of constant width W, which allows an analytical solution for the penetration distance L; we therefore are not modeling the narrow strait that commonly constricts the entrance to nearly-enclosed seas on the modern Earth, such as the Bab al Mandeb, the Strait of Gibraltar, and the Bosporus. In this model, the length-to-width ratio L/W at which the ice thickness diminishes to zero just at the far end of the narrow sea is a function of just three variables: the thickness H_0 at the entrance, the net sublimation rate at the top surface $\dot{b}$ (positive where sublimation exceeds precipitation), and the atmospheric temperature T_s (which determines the ice temperature and effective ice softness and thus the flow velocity). We assume that there is no melting or freezing at the base of the sea glacier tongue. If the climate in the refugium is warm enough to support open water, there might be melting at the surface or base of the glacier, which would reduce L and make the probability of a refugium more likely than our computations here suggest.

2. Why Inland Seas Could Protect Refugia From Sea Glaciers

[5] The flow of a sea glacier into a channel would be resisted by drag stress along the sidewalls of the channel. If this channel is located in a region of net sublimation, the

[1]Department of Earth and Space Sciences, University of Washington, Seattle, Washington, USA.
[2]Astrobiology Program, University of Washington, Seattle, Washington, USA.

0094-8276/11/2011GL048846

inflowing sea glacier will lose mass as it invades the channel. Alternatively, if the narrow sea is in a region of net accumulation, it would be surrounded by glaciated land and filled with snow-covered ice; thus an inland sea can provide a refugium only if it is in a region of net sublimation; i.e., surrounded by extensive desert. If the channel is sufficiently narrow, the resistive drag stresses impede the inflowing sea glacier, and sublimation causes the sea glacier to shrink to zero thickness after some length L.

[6] In order for an inland sea to provide a refugium for photosynthetic organisms during snowball events, several conditions must have been satisfied: (1) the inland sea must not be fully penetrated by a sea glacier; (2) the climate on the inland sea must be such as to maintain it either ice-free or covered by an ice layer sufficiently thin to allow photosynthesis below the ice; (3) the depth of the sea at its entrance, and throughout its length, must be great enough that seawater is able to flow under the sea glacier to replenish water loss from the refugium by evaporation/sublimation, and (4) water circulation in the inland sea must be adequate to allow nutrients to be delivered to organisms living in the bay at the landward end. Here, during this first exercise, we examine only the first condition.

3. Penetration Length of Sea Glaciers

[7] In order to determine whether inland seas could have remained free of sea-glacier ice, we estimate the penetration length L of a sea glacier flowing into an inland sea. The penetration length is defined as the distance a sea glacier, with an initial thickness H_0, would have traveled before reaching zero thickness. To determine the penetration length L we derive an analytical solution for flow along a parallel-sided channel using force balance and continuity. *Weertman* [1957] determined the creep rate for an unconfined ice shelf with a uniform thickness and width. *Thomas* [1973] expanded on the work of *Weertman* [1957] by considering the creep rate of a confined ice shelf. By assuming a yield stress for sidewall shearing, he concluded that velocity in the downstream direction is constant. *Sanderson* [1979] found that velocity in the downstream direction did vary, but the variation was small. Therefore, we will assume that velocity is uniform in the downstream direction.

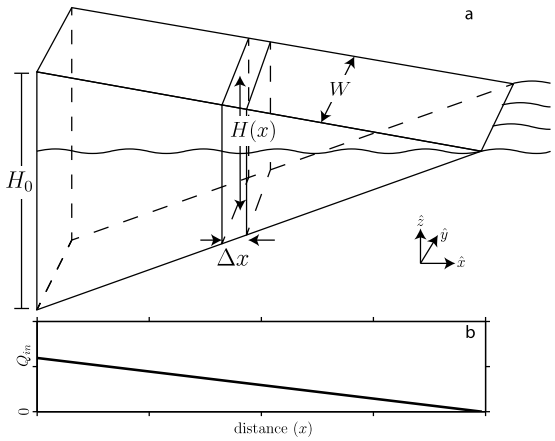

Figure 1. Cartoon schematic of a sea glacier penetrating a channel. (a) Ice thickness. (b) Ice flux. Both decrease linearly with distance, while mean across-channel velocity $\overline{u}$ is uniform along the channel.

Table 1. Constants Used in Analysis

Name	Symbol	Value	Units
Temperature-independent ice softness parameter	A_0	4×10^{-13}	$Pa^{-3}\ s^{-1}$
Clausius-Clapeyron exponent	G	51	kJ/mol
acceleration of gravity	g	9.81	m/s^2
flow law exponent	n	3	dimensionless
activation energy for creep	Q_c	60	kJ/mol
ideal gas constant	R	8.314	$J\ mol^{-1}\ K^{-1}$
ice density	ρ_i	917	kg/m^3
seawater density	ρ_w	1043	kg/m^3

[8] Consider a sea glacier that enters a narrow channel with a uniform width W and vertical walls (Figure 1a). We choose the x-direction to be horizontal and parallel to the channel walls, the y-direction to be perpendicular to the channel walls, and the z-direction to be vertical, positive upward. The centerline of the sea glacier is at $y = 0$.

[9] Environmental controls such as temperature and net rate of sublimation also control the penetration length of a sea glacier. In Snowball Earth models, zonally-averaged mean annual surface temperatures ranged from −50°C to −20°C at latitudes where net sublimation was likely [*Goodman*, 2006; *Pierrehumbert et al.*, 2011]. Ice is softer at warmer temperatures, hence a warmer sea glacier will flow faster so may penetrate farther. Basal temperatures were calculated by adjusting the melting point of ice for pressure and salt content. Salt content was estimated by assuming present-day total salinity and total volume of the ocean, and adjusting the salinity taking into account the salt-free ice covering the ocean during a Snowball Earth event. A relationship between ice temperature and the softness parameter $A(T)$ has been derived empirically [*Cuffey and Paterson*, 2010, p. 75] and has a functional form

$$A(T) = A_0 \exp\left(\frac{-Q_c}{RT}\right) \tag{1}$$

where A_0 represents a temperature-independent softness coefficient, Q_c represents the activation energy for creep, R represents the ideal gas constant, and T represents ice temperature. Values for the constants are given in Table 1. Because the rate of vertical advection of heat is small compared to the heat conduction rate, we assume a linear temperature profile throughout the ice thickness. Then we calculate an effective isothermal ice softness parameter A that satisfies force balance and produces the same ice flux in the channel as the value obtained by using the nonuniform temperature profile; a full explanation is given in the auxiliary material.[1] This new isothermal ice softness parameter A is used in place of the depth-dependent A in all equations that follow. Using an effective isothermal ice temperature to determine ice softness allows us to solve the problem using simpler isothermal equations.

[10] The mass loss has two components, sublimation at the surface of the sea glacier, and melting at its base where

[1] Auxiliary materials are available in the HTML. doi:10.1029/2011GL048846.

it contacts ocean water. The net rate of sublimation, $\dot{b}$, is poorly constrained. In *Pierrehumbert*'s [2005] model [see also *Pierrehumbert et al.*, 2011, Figure 7], the zonal average net sublimation rate peaked at the equator with a value of 5 mm/year, for 2000 ppm CO_2. During the coldest phase of a Snowball Earth event, CO_2 may have been just 100 ppm, and corresponding net sublimation only 3 mm/year [*Pierrehumbert*, 2005, Figure 10]. *Goodman* [2006] calculated that mass loss through basal melting is insignificant compared to sublimation losses at equatorial latitudes. Therefore we use a parameter space to calculate penetration lengths where net rate of sublimation and ice softness are varied, while other parameters are held constant (Table 1).

3.1. Channel Velocity

[11] *Nye* [1965] solved for the velocity for a glacier with infinite depth and uniform width W where flow is resisted by two parallel sidewalls. Nye's equation 7 neglected vertical shearing because of the infinite thickness of the glacier. A sea glacier entering a narrow channel does not undergo vertical shearing because the sea glacier is floating and water cannot support a shear stress, so Nye's solution is appropriate:

$$u(x,y) = \frac{W}{2}\frac{A(x)k(x)^n}{n+1}\left(1 - \left|\frac{2y}{W}\right|^{n+1}\right) \tag{2}$$

where u represents velocity in the x-direction, k represents resistive drag stress at the walls, A represents ice softness, and n represents the exponent in the Glen ice flow law [*Glen*, 1955]. Nye's solution assumes no variation of velocity in the x-direction, but variation of u in the x-direction is permitted if k varies as a function of x. Variation of k in the z-direction is not permitted, because there is no basal shear stress to cause a vertical gradient of velocity. Equation (2) can be integrated across the channel to calculate a mean velocity, $\overline{u}(x)$

$$\overline{u}(x) = \frac{W}{2}\frac{A(x)k(x)^n}{n+2} \tag{3}$$

3.2. Continuity

[12] We use the time-independent mass conservation equation

$$\nabla \cdot (\overline{\mathbf{u}}H) + \dot{b} = 0, \tag{4}$$

where $\overline{\mathbf{u}}$ represents the ice-velocity vector, H represents local ice thickness, and $\dot{b}$ represents the net sublimation rate at the upper surface ($\dot{b}$ is positive for loss in volume). Motion is entirely in the x-direction, so equation (4) can be written as

$$\frac{\mathrm{d}\overline{u}}{\mathrm{d}x}H(x) + \overline{u}(x)\frac{\mathrm{d}H}{\mathrm{d}x} = -\dot{b}(x) \tag{5}$$

Substituting equation (3) into equation (5) results in

$$H(x)\frac{W}{2}\frac{A(x)}{n+2}\frac{\mathrm{d}}{\mathrm{d}x}(k(x)^n) + \frac{W}{2}\frac{A(x)k(x)^n}{n+2}\frac{\mathrm{d}H}{\mathrm{d}x} = -\dot{b}(x) \tag{6}$$

3.3. Force Balance

[13] To solve equation (6), we must determine the resistive drag stress k as a function of x. We use a force-balance approach where we assume that the pressure gradient forces in a sea glacier flowing along a narrow channel are entirely balanced by the resistive drag force at the sides; a full explanation is given in the auxiliary material, where equation (S12) shows that the resistive drag stress at the walls is

$$k(x) = -\frac{W}{2}\Gamma\frac{\mathrm{d}H}{\mathrm{d}x} \tag{7}$$

where Γ is defined as

$$\Gamma \equiv \rho_i g\left(1 - \frac{\rho_i}{\rho_w}\right) \tag{8}$$

and ρ_i represents the density of ice, ρ_w represents the density of sea water, and g represents the acceleration due to gravity. By substituting equation (7) into equation (6), we can write a differential equation in terms of H

$$\frac{W}{2}\frac{A(x)}{n+2}\left(\frac{-W}{2}\Gamma\right)^n\left[nH(x)\left(\frac{\mathrm{d}H}{\mathrm{d}x}\right)^{n-1}\frac{\mathrm{d}^2H}{\mathrm{d}x^2} + \left(\frac{\mathrm{d}H}{\mathrm{d}x}\right)^{n+1}\right] = -\dot{b}(x) \tag{9}$$

Equation (9) with the boundary condition $H(0) = H_0$ has a solution in which H varies linearly with x:

$$H(x) = H_0\left(1 - \frac{x}{L}\right) \tag{10}$$

$$\frac{\mathrm{d}H}{\mathrm{d}x} = -\frac{H_0}{L} \tag{11}$$

$$\frac{\mathrm{d}^2H}{\mathrm{d}x^2} = 0 \tag{12}$$

The ratio L/W can be found by substituting equations (10), (11), and (12) into equation (6) to get

$$\frac{L}{W} = \frac{H_0}{D} \tag{13}$$

where

$$D = 2\left(\frac{\dot{b}(n+2)}{A\Gamma^n}\right)^{\frac{1}{n+1}} \tag{14}$$

is a characteristic length that depends on temperature, through A, and net sublimation rate $\dot{b}$.

[14] Mean velocity, $\overline{u}$, across the channel can be calculated as

$$\overline{u} = \frac{W}{2}\left(\frac{A(\Gamma\dot{b})^n}{n+2}\right)^{\frac{1}{n+1}} \tag{15}$$

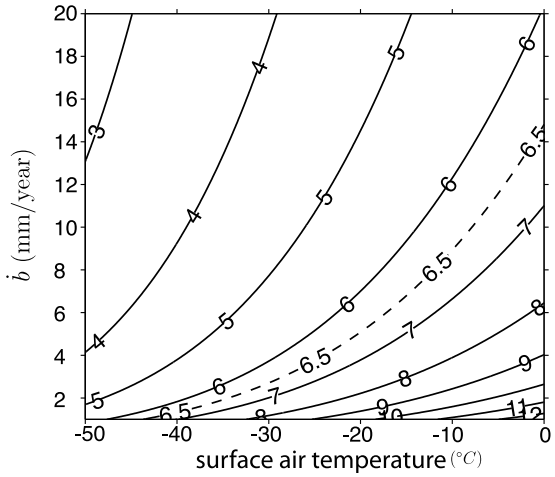

Figure 2. Solid contours represent penetration length-to-width ratio L/W as a function of net sublimation rate $\dot{b}$ and surface ice temperature T_s for a sea glacier with an initial thickness H_0 = 650 m, entering a narrow channel. Dashed line represents the 6.5 L/W ratio for the Red Sea. Atmospheric conditions to the left of the dashed line allow a refugium to avoid being over-ridden at the end of the Red Sea analogue.

and flux, Q_0, entering the channel through the upstream end from the global sea glacier can be calculated as

$$Q_0 = WH_0\overline{u}. \tag{16}$$

4. Application to a Modern Analogue

[15] Penetration length scales linearly with channel width (equation (13)); therefore, penetration length L can be non-dimensionalized in terms of channel width W. Figure 2 demonstrates that a sea glacier can penetrate farther into a narrow channel if it has lower net sublimation rate $\dot{b}$, and/or warmer air temperatures represented by larger ice softness parameter A.

[16] As a characteristic inland sea we use the Red Sea, a nearly enclosed basin in the Red Sea Rift, a spreading center between the African and Arabian plates. Because the rifting of continental plates is caused by convection in the Earth's mantle, which was presumably not significantly affected by Snowball Earth events, it is reasonable to assume that inland seas like the Red Sea existed during Snowball Earth events.

[17] To determine the penetration length of a sea glacier moving into a Red Sea analogue, we approximate the sea by a rectangle 200 km wide and 1300 km long; the length-to-width ratio L/W is 6.5. We assume that the upstream thickness H_0 of a sea glacier at the mouth of a Red Sea analogue is 650 m, consistent with ice thickness of the global sea glacier in regions of net sublimation [*Goodman*, 2006]; however, penetration length scales linearly with H_0 (equation (13)) so a thicker global sea glacier could penetrate proportionally farther. The length of the Red Sea exceeds the penetration length of the sea glacier if the combination of ice temperature and sublimation rate falls to the left of the dashed line in Figure 2. The along-channel ice thickness $H(x)$, and ice flux $Q(x)$ for a sea glacier, decrease linearly with distance Figure 1 while mean along-channel velocity $\overline{u}$ remains constant.

[18] The planetary climate of a Snowball Earth event warms over time through either the build-up of atmospheric CO_2 or changes in planetary albedo [*Abbot and Pierrehumbert*, 2010]. As the planet warms, the length-to-width ratio L/W of a sea glacier invading a narrow channel may change. We explore changes in L/W by exploring changes in the local net sublimation rate $\dot{b}$ and ice softness A due to a change in atmospheric temperature T_s. Here, we assume that changes $\dot{b}$ are proportional to changes in the saturation vapor pressure from a Clausius-Clapeyron relation

$$\dot{b}(T_s) = c\ \exp\left(\frac{-G}{T_s R}\right) \tag{17}$$

where c represents a constant based on initial conditions, and G represents the Clausius-Clapeyron exponent from *Marti and Mauersberger* [1993]. Atmospheric temperature T_s changes slowly enough to allow the sea glacier to always be in an equilibrium steady-state because the time scale of thermal diffusion in the penetrating sea glacier is much less than the time scale for global changes in T_s. Therefore T_s can be used as a proxy for time. Figure 3a shows an example calculation with initial climate conditions of $T_s = -50$°C and $\dot{b}$ = 1 mm/year. The length-to-width ratio L/W of the sea glacier, described by equation (13), decreases in a warming world because increases in length due to increased ice softness are smaller than decreases in length due to increased net sublimation (Figure 3b). Both sublimation and shearing

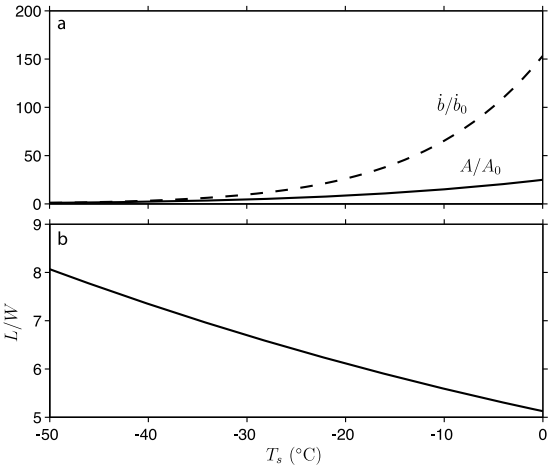

Figure 3. (a) How increasing atmospheric temperatures during deglaciation affect net sublimation rate $\dot{b}$, relative to an initial value $\dot{b}_0$ of 1 mm/year (dashed line), and ice softness A, relative to an initial value A_0 set by a surface temperature $T_s = -50$°C (solid line). Net sublimation rate $\dot{b}$ is more sensitive than ice softness A to rising surface temperature T_s. (b) Resulting length-to-width ratio L/W of a invading sea glacier, calculated from equation (13). For this particular example, the initial upstream ice thickness is H_0 = 650 m.

require breaking of hydrogen bonds. Correspondingly, the Clausius-Clapeyron exponent (51 kJ/mol) is similar to the activation energy for creep (60 kJ/mol); each is approximately the energy required to break two hydrogen bonds. The reason that A increases more slowly than $\dot{b}$ in Figure 3b is that $\dot{b}$ is determined by the surface temperature whereas A is determined by an effective depth-averaged temperature including the influence of warm ice at the bottom (−2°C) for all values of the surface temperature. Although this is a specific example, other reasonable initial conditions produce qualitatively similar results. In addition, this approach does not take into account surface and basal melting processes that would be expected once atmospheric conditions are near the melting temperature, and furthermore the upstream thickness H_0 of the global sea glacier entering the channel would decrease in a warming world. Both of these effects would decrease L/W for an invading sea glacier and L/W would be less than its initial value throughout the deglaciation.

5. Conclusions

[19] As modeled here, an analogue to the Red Sea is long enough to have provided a refugium for photosynthetic organisms during Snowball Earth events, only if certain surface temperature and net sublimation conditions were met. The penetration length of an invading sea glacier continuously decreases as the planet warms during a Snowball Earth event. In future work, the restraining effect of a narrow entrance strait to the sea will be considered. That investigation will require a numerical model, but will likely allow a refugium to exist over a wider range of atmospheric temperatures and net sublimation rates.

[20] **Acknowledgments.** This work was supported by NSF grant ANT-0739779. We thank John Booker for suggesting that we search for an analytical solution. We thank Matt Smith, Dorian Abbot, Raymond Pierrehumbert and an anonymous reviewer for their very helpful comments.

[21] The Editor thanks Dorian Abbot, Raymond Pierrehumbert and an anonymous reviewer for their assistance in evaluating this paper.

References

Abbot, D. S., and R. T. Pierrehumbert (2010), Mudball: Surface dust and Snowball Earth deglaciation, *J. Geophys. Res.*, *115*, D03104, doi:10.1029/2009JD012007.

Cuffey, K. M., and W. S. B. Paterson (2010), *The Physics of Glaciers*, 4th ed., 693 pp., Elsevier, Amsterdam.

Evans, D. A. D. (2000), Stratigraphic, geochronological, and paleomagnetic constraints upon the Neoproterozoic climatic paradox, *Am. J. Sci.*, *300*, 347–433.

Glen, J. (1955), The creep of polycrystalline ice, *Proc. R. Soc. A*, *228*, 519–538.

Goodman, J. C. (2006), Through thick and thin: Marine and meteoric ice in a "Snowball Earth" climate, *Geophys. Res. Lett.*, *33*, L16701, doi:10.1029/2006GL026840.

Goodman, J. C., and R. T. Pierrehumbert (2003), Glacial flow of floating marine ice in "Snowball Earth," *J. Geophys. Res.*, *108*(C10), 3308, doi:10.1029/2002JC001471.

Harland, W. (1964), Critical evidence for a great infra-Cambrian glaciation, *Geol. Rundsch.*, *54*, 45–61, doi:10.1007/BF01821169.

Hoffman, P. F., and D. P. Schrag (2000), Snowball Earth, *Sci. Am.*, *282*(1), 68–75.

Hoffman, P. F., A. J. Kaufman, G. P. Halverson, and D. P. Schrag (1998), A Neoproterozoic Snowball Earth, *Science*, *281*, 1342–1346, doi:10.1126/science.281.5381.1342.

Kirschvink, J. L. (1992), Late Proterozoic low-latitude global glaciation: The Snowball Earth, in *The Proterozoic Biosphere*, chap. 2.3, pp. 51–52, Cambridge Univ. Press, New York.

Knoll, A. (1992), The early evolution of eukaryotes: A geological perspective, *Science*, *256*, 622–627, doi:10.1126/science.1585174.

Macdonald, F. A., M. D. Schmitz, J. L. Crowley, C. F. Roots, D. S. Jones, A. C. Maloof, J. V. Strauss, P. A. Cohen, D. T. Johnston, and D. P. Schrag (2010), Calibrating the Cryogenian, *Science*, *327*, 1241–1243, doi:10.1126/science.1183325.

Marti, J., and K. Mauersberger (1993), A survey and new measurements of ice vapor pressure at temperatures between 170 and 250K, *Geophys. Res. Lett.*, *20*(5), 363–366.

Nye, J. F. (1965), The flow of a glacier in a channel of rectangular, elliptical or parabolic cross-section, *J. Glaciol.*, *5*, 661–690.

Pierrehumbert, R. T. (2005), Climate dynamics of a hard snowball Earth, *J. Geophys. Res.*, *110*, D01111, doi:10.1029/2004JD005162.

Pierrehumbert, R. T., D. Abbot, A. Voigt, and D. Koll (2011), Climate of the Neoproterozoic, *Annu. Rev. Earth Planet. Sci.*, *39*, 417–460, doi:10.1146/annurev-earth-040809-152447.

Pollard, D., and J. F. Kasting (2005), Snowball Earth: A thin-ice solution with flowing sea glaciers, *J. Geophys. Res.*, *110*, C07010, doi:10.1029/2004JC002525.

Pollard, D., and J. F. Kasting (2006), Reply to comment by Stephen G. Warren and Richard E. Brandt on "Snowball Earth: A thin-ice solution with flowing sea glaciers," *J. Geophys. Res.*, *111*, C09017, doi:10.1029/2006JC003488.

Sanderson, T. J. O. (1979), Equilibrium profile of ice shelves, *J. Glaciol.*, *22*, 435–460.

Thomas, R. H. (1973), The creep of ice shelves: Theory, *J. Glaciol.*, *12*, 45–53.

Warren, S. G., R. E. Brandt, T. C. Grenfell, and C. P. McKay (2002), Snowball Earth: Ice thickness on the tropical ocean, *J. Geophys. Res.*, *107*(C10), 3167, doi:10.1029/2001JC001123.

Weertman, J. (1957), Deformation of floating ice shelves, *J. Glaciol.*, *3*, 38–42.

A. J. Campbell, E. D. Waddington, and S. G. Warren, Department of Earth and Space Sciences, University of Washington, Box 351310, Seattle, WA 98195-1310, USA. (campbead@uw.edu; edw@uw.edu; sgw@uw.edu)

Calculation of resistive drag stress

In order to calculate the resistive drag stress k along the sidewall of a sea glacier flowing through a narrow channel, a force-balance technique is used. Consider a vertical section of a sea glacier (Figure S-1) flowing through a narrow channel of uniform width W. The section has infinitesimal length Δx, where the thickness of the upstream and downstream ends are represented by H_U and H_D respectively. Pressure from ice at the upstream end P_U, acts to push the ice block downstream, while pressure from ice at the downstream end P_D, pressure from seawater P_{SW}, and resistive drag stress k from the sidewalls all act to resist the downstream motion of the ice block. We assume that the sea glacier is not accelerating, and that only pressure and drag forces act on the glacier, so that

$$F_U + F_D + F_{SW} + F_R = 0 \tag{S-1}$$

where F_U, F_D and, F_{SW} respectively represent forces due to pressure applied from ice at the upstream end, from ice at the downstream end, and from sea water at the base, and F_R represents the resistive drag force applied by the sidewalls. We assume that the stress deviator in the x-direction is zero, meaning that the compressive stress in the x-direction is due to ice pressure. This assumption leads to our uniform velocity, $\bar{u}$. *Sanderson*

[1979] found that the along-channel velocity is uniform for an ice shelf moving through a parallel-sided bay when he assumed a constant resistive drag stress k.

Pressure forces are calculated by integrating pressure over the appropriate face. Pressure at the upstream end of the section is linear with depth

$$P_U(z) = \Gamma \left(H_U \left(1 - \frac{\rho_i}{\rho_w} \right) - z \right) \tag{S-2}$$

where Γ is defined

$$\Gamma \equiv \rho_i g \left(1 - \frac{\rho_i}{\rho_w} \right) \tag{S-3}$$

Here, z is positive upward and sea level is at $z = 0$. The force applied at the upstream end of the thin cross-sectional element from pressure is calculated by integration over the upstream face

$$F_U = \int_{-H_U\left(\frac{\rho_i}{\rho_w}\right)}^{H_U\left(1-\frac{\rho_i}{\rho_w}\right)} \int_{-W/2}^{W/2} P_U(z)\,\mathrm{d}y\,\mathrm{d}z = \frac{W}{2}\rho_i g H_U^2 \tag{S-4}$$

Force at the downstream end is calculated similarly

$$F_D = -\frac{W}{2}\rho_i g H_D^2 \tag{S-5}$$

where a negative sign indicates force acting in the upstream direction.

Pressure of the sea water is linear with depth below sea level

$$P_{SW}(z) = \rho_w g(-z) \tag{S-6}$$

The component of force due to the pressure of seawater directed horizontally is calculated by integrating over the face from the base of the downstream end, to the base of the upstream end of the section.

$$F_{SW} = \int_{-H_U\left(\frac{\rho_i}{\rho_w}\right)}^{-H_D\left(\frac{\rho_i}{\rho_w}\right)} \int_{-W/2}^{W/2} P_{SW}(z)\,\mathrm{d}y\,\mathrm{d}z = -\frac{W}{2}\rho_i g\left(\frac{\rho_i}{\rho_w}\right)(H_U^2 - H_D^2) \tag{S-7}$$

where a negative sign indicates force acting in the upstream direction.

Substitution of Equations S-4, S-5, and S-7 into Equation S-1 yields

$$F_R = -\frac{W}{2}\Gamma[H_U^2 - H_D^2] \tag{S-8}$$

H_D can be described as a first-order Taylor expansion about H_0

$$H_D = H_U + \frac{\mathrm{d}H}{\mathrm{d}x}\Big|_{x_U}\Delta x \tag{S-9}$$

where the upstream face is at $x = x_U$

Substitution of Equation S-9 into Equation S-8 yields

$$F_R = -\frac{W}{2}\Gamma\left[-2H_U\frac{\mathrm{d}H}{\mathrm{d}x}\Delta x + \left(\frac{\mathrm{d}H}{\mathrm{d}x}\Delta x\right)^2\right]. \tag{S-10}$$

Since Δx is very small we can neglect terms containing $(\Delta x)^2$, and

$$F_R \approx W H_U \Gamma \frac{\mathrm{d}H}{\mathrm{d}x}\Delta x. \tag{S-11}$$

The resistive drag force along the two sidewalls is the integral of the resistive drag stress k over the sidewalls, where a negative sign indicates force acting in the upstream direction:

$$F_R = -2\int_x^{x+\Delta x}\int_0^{H(x)} k(x)\,\mathrm{d}z\,\mathrm{d}x = 2k(x)H(x)\Delta x. \tag{S-12}$$

We can now substitute Equation S-11 into Equation S-12 to calculate resistive drag stress:

$$k(x) = -\frac{W}{2}\Gamma\frac{\mathrm{d}H}{\mathrm{d}x}, \tag{S-13}$$

which turns out to be uniform in our analysis.

Calculation of effective softness and temperature

Our analytical solution (Equations 13 and 14) for the sea-glacier profile in an embayment requires isothermal ice. From Equations 3, 7, and 16, the isothermal ice flux through the cross-section at x is given by

$$Q_{iso}(x) = \frac{-A(x)}{2(n+2)}\left(\frac{W}{2}\Gamma\left|\frac{\mathrm{d}H}{\mathrm{d}x}\right|\right)^n W^2 H(x). \tag{S-14}$$

However, on Snowball Earth, the basal temperature would have been at the freezing point of seawater (approximately -2°C), while the upper surface was at the ambient air temperature T_s, so A then also had a strong depth dependence. When temperature varies with depth, the velocity profile across the channel at any depth z is still described by a form of Equation 2,

$$u(x,y,z) = \frac{W}{2}\frac{A(x,z)k(x,z)^n}{(n+2)}\left(1-\left|\frac{2y}{W}\right|^{n+1}\right). \tag{S-15}$$

With the assumption that vertical shear is negligible, i.e.

$$\frac{\partial u}{\partial z} = 0 \tag{S-16}$$

the cold upper ice acts as a stress guide, and wall drag $k(x, z)$ must be larger in the cold ice where softness $A(x, z)$ is smaller, so that

$$A(x, z)k(x)^n = C \tag{S-17}$$

where C is a constant that can be determined. The softness $A(x, z)$ is known from the temperature profile, and the depth-averaged value of $k(x, z)$ must equal the value of $k(x)$ in Equation 7 in the isothermal case for the same sea-glacier geometry, in order to balance the forces in Equation S-1. As a result,

$$C = \left[\frac{-\frac{W}{2}\Gamma \left|\frac{\mathrm{d}H}{\mathrm{d}x}\right|}{\frac{1}{H(x)} \int_0^{H(x)} A(x, \zeta)^{-1/n} \mathrm{d}\zeta} \right]^n \tag{S-18}$$

and the ice flux can be written as

$$Q(x) = WH(x)\bar{u}(x) = \frac{W^2}{2(n+2)} H(x)C = \frac{-W^2 H(x)}{2(n+2)} \left(\frac{W}{2}\Gamma \left|\frac{\mathrm{d}H}{\mathrm{d}x}\right|\right)^n \left(\frac{1}{H(x)} \int_0^{H(x)} A(x, \zeta)^{-1/n} \mathrm{d}\zeta\right)^{-n}. \tag{S-19}$$

The depth integral can be evaluated numerically from the known temperature profile $T(x, z)$ and Equation 1. We can then define an effective ice softness $A_{eff}(x)$for the cross-section as

$$A_{eff}(x) = \left(\frac{1}{H(x)} \int_0^{H(x)} A(x, \zeta)^{-1/n} \mathrm{d}\zeta\right)^{-n}. \tag{S-20}$$

With the substitution Equation S-20, Equation S-19 takes the same form as Equation S-14, so ice flux through any cross-section in a non isothermal sea glacier can be calculated correctly with the isothermal Equations 15 and 16, by replacing $A(x)$ with $A_{eff}(x)$ from Equation S-20.

Furthermore, when the temperature profile is linear with depth, and the surface temperature T_s is spatially uniform, A_{eff} is independent of ice thickness $H(x)$, and so is also independent of x. A uniform effective temperature T_{eff} for the entire sea glacier can then be derived from A_{eff} through Equation 1.

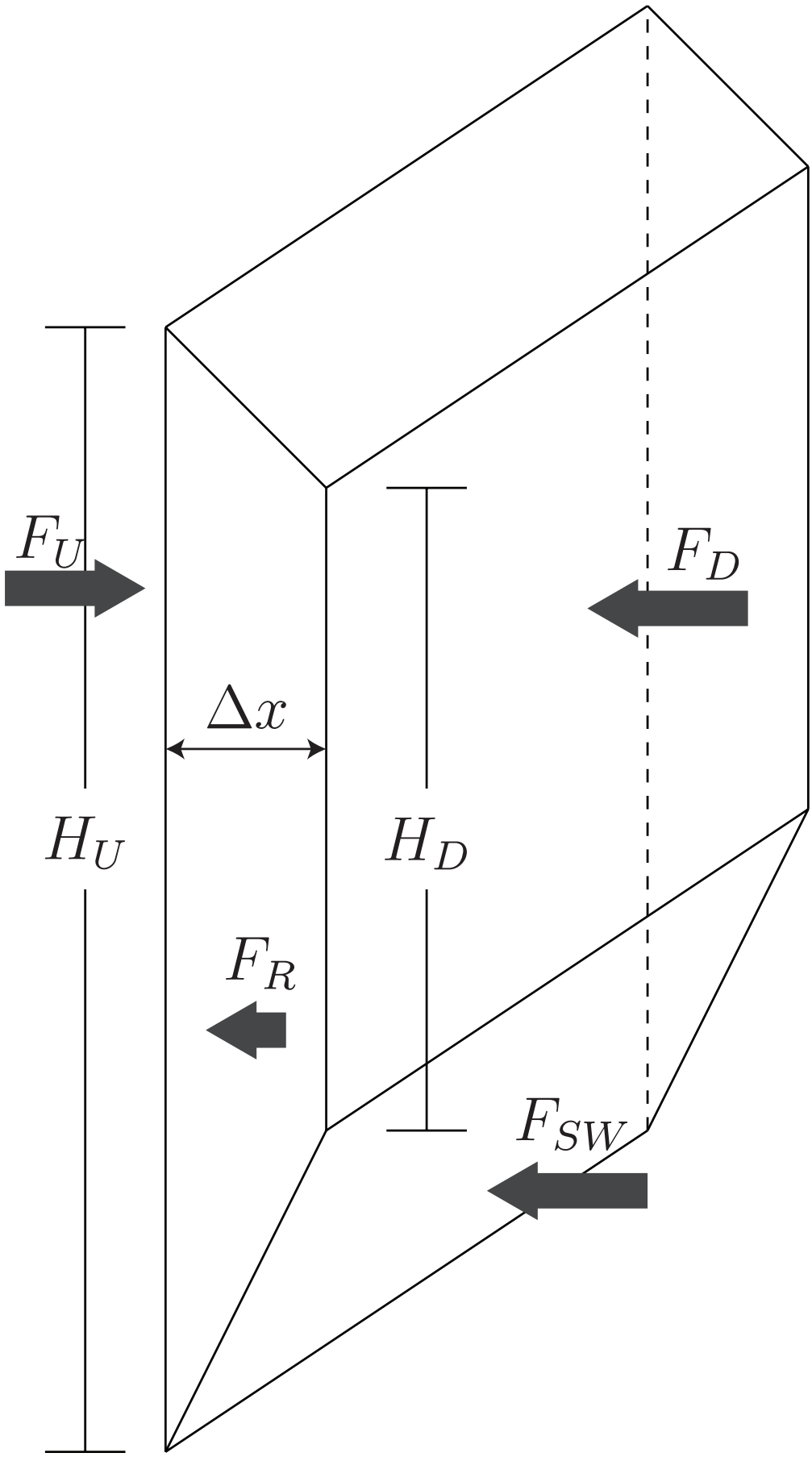
F_U
F_D
Δx
H_U
H_D
F_R
F_{SW}

Figure S-1. A section of a sea glacier penetrating a channel experience forces acting on the upstream face from the pressure of ice F_U, on the downstream face from the pressure of ice F_D, on the basal face from the pressure of seawater F_{SW}, and on the sidewalls from drag resistance F_R.

Chapter 4

REFUGIUM FOR SURFACE LIFE ON SNOWBALL EARTH IN A NEARLY ENCLOSED SEA? A NUMERICAL SOLUTION FOR SEA-GLACIER INVASION THROUGH A NARROW STRAIT

Originally published in Journal of Geophysical Research: Oceans

Adam J. Campbell, Edwin D. Waddington, and Stephen G. Warren. Refugium for surface life on Snowball Earth in a nearly enclosed sea? A numerical solution for sea- glacier invasion through a narrow strait. *Journal of Geophysical Research: Oceans*, 119 (4):26792690, 2014. doi: 10.1002/2013JC009703.

This second paper considers ice moving through a narrow entrance into an inland sea. Previously we suggested that a narrow entrance to a channel would diminish the ability of a sea glacier to invade a channel. In this work, I developed a 2-D ice flow model suitable for floating ice. This new model allowed us to capture additional physics into our sea-glaicer flow model that the previous model was unable to consider. It also allowed us to experiment with geometries that were more complex than the previous studied, which was limited to channels with parallel-sided walls of a uniform width. The inclusion of a narrow entrance expanded the range of climate conditions allowing for incomplete sea-glacier penetration. When the model was coupled to a thermal evolution model it demonstrated that sea-glacier penetration diminishes with increasing surface temperatures over time. We also explored the case of a sea glacier penetrating a channel that is colder at its entrance and warmer at its interior. The scenario is possible for a sea glacier being warmed by invading a channel surrounded by desert land.

This paper confirmed our previous analytical model in a more robust manner. It demonstrated that the previous model was an upper bound for sea-glacier penetration. The model produced sea-glacier-free zones that were not initially expected. We hypothesized these zones could form downstream of promontories or islands, inspiring our next work.

For this work, I developed the solution for ice-flow model and calculated the change in ice penetration during a warming Snowball Earth. E. D. Waddington provided support for ice-flow modeling and developed the initial code for the thermal evolution model. S. G. Warren helped provide much of the background context of Snowball Earth.

AGU PUBLICATIONS

JGR

Journal of Geophysical Research: Oceans

RESEARCH ARTICLE
10.1002/2013JC009703

Key Points:
- Inland seas could have been refugia for life during Snowball Earth events
- Narrow entrances of inland sea restrict the flow of invading sea glaciers
- Sea-glacier-free zones may have existed near narrow entrances

Correspondence to:
A. J. Campbell,
campbead@uw.edu

Citation:
Campbell, A. J., E. D. Waddington, and S. G. Warren (2014), Refugium for surface life on Snowball Earth in a nearly enclosed sea? A numerical solution for sea-glacier invasion through a narrow strait, *J. Geophys. Res. Oceans*, *119*, doi:10.1002/2013JC009703.

Received 5 DEC 2013
Accepted 4 APR 2014
Accepted article online 8 APR 2014

Refugium for surface life on Snowball Earth in a nearly enclosed sea? A numerical solution for sea-glacier invasion through a narrow strait

Adam J. Campbell[1], Edwin D. Waddington[1], and Stephen G. Warren[1,2]

[1]Department of Earth and Space Sciences, University of Washington, Seattle, Washington, USA, [2]Astrobiology Program, University of Washington, Seattle, Washington, USA

Abstract Where photosynthetic eukaryotic organisms survived during the Snowball Earth events of the Neoproterozoic remains unclear. Our previous research tested whether a narrow arm of the ocean, similar to the modern Red Sea, could have been a refugium for photosynthetic eukaryotes during the Snowball Earth. Using an analytical ice-flow model, we demonstrated that a limited range of climate conditions could restrict sea-glacier flow sufficiently to allow an arm of the sea to remain partially free from sea-glacier penetration, a necessary condition for it to act as a refugium. Here we expand on the previous study, using a numerical ice-flow model, with the ability to capture additional physics, to calculate sea-glacier penetration, and to explore the effect of a channel with a narrow entrance. The climatic conditions are made self-consistent by linking sublimation rate to surface temperature. As expected, the narrow entrance allows parts of the nearly enclosed sea to remain safe from sea-glacier penetration for a wider range of climate conditions.

1. Introduction

During the "Snowball Earth" events of the Neoproterozoic, approximately 600–800 Ma [*Hoffman and Schrag*, 2002], the entire upper ocean surface may have been covered with "sea glaciers," ice several hundreds of meters thick that are thick enough to deform under their own weight [*Goodman and Pierrehumbert*, 2003; *Goodman*, 2006; *Li and Pierrehumbert*, 2011]. Photosynthetic eukaryotic algae existed immediately prior to and after these events [*Knoll*, 1992; *Macdonald et al*., 2010] so they are presumed to have survived during Snowball Earth. These algae require both liquid water and sunlight. Our previous research [*Campbell et al*., 2011] explored the ability of a nearly enclosed sea, connected to the ocean by a narrow channel, to provide a refugium for photosynthetic eukaryotic life during a Snowball Earth event. (Figure 1 provides an illustration of how we envision a sea-glacier penetrating into an inland sea.) We demonstrated, using an analytical solution of momentum balance and continuity equations, that the landward end of the sea could remain free from sea-glacier penetration, provided particular geometric and climatic conditions existed. If an inland sea is not fully penetrated by a sea glacier, then it has achieved one of the conditions needed to provide a refugium for photosynthetic eukaryotic life. In addition, the sea would have to be located in a desert region, where evaporation/sublimation exceeds precipitation, and the refugium's temperature would have to be warm enough that thick sea ice did not grow locally. The flow of ice through constrictions was also studied by *Tziperman et al*. [2012].

Section 2 reviews the previously developed model of sea-glacier penetration of *Campbell et al*. [2011]. Section 3 describes the newly developed numerical model of sea-glacier penetration. That section includes descriptions of the model's body equations, boundary conditions, and parameters, as well as modifications made to the model to ensure numerical stability, and our solution scheme. Section 4 describes the two experiments performed using the numerical model: a comparison experiment where we compare the new model results to those of *Campbell et al*. [2011] and an experiment where we vary the entrance width of the channel. Section 5 describes an experiment in which we couple a thermal evolution model to the sea-glacier flow model to demonstrate that sea-glacier penetration is reduced in a channel that is warmer at its far end than at its entrance, in accord with the climate necessary to prevent sea-ice growth locally at the far end. In section 6, we discuss the results and assumptions of the experiments, including the discovery of upstream sea-glacier-free zones, the atmospheric constraints that would be required for incomplete

AGU Journal of Geophysical Research: Oceans 10.1002/2013JC009703

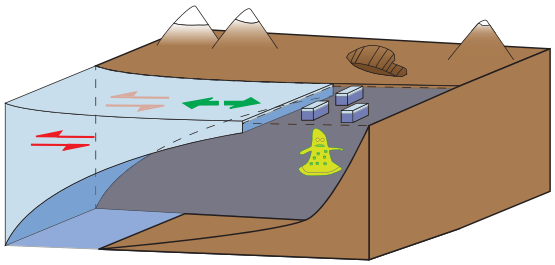

Figure 1. As a sea glacier invades into an inland sea, the flow of the sea glacier is restricted by lateral shear (red arrows) and longitudinal stretching (green arrows). Inland seas located near the equator would be in regions of net sublimation. In a region of net sublimation, the ground would be bare, except at the highest altitudes. Lakes would be unable to provide refugia for photosynthetic algae because a modest sublimation rate would be able to completely dry out even the deepest lakes known during the estimated several-million-year duration of a Snowball Earth event.

sea-glacier penetration, and our choice to not address the effect of submarine melting. Section 7 summarizes our conclusions that narrow entrances widen the range of climate conditions that allow for inland seas to act as refugia for photosynthetic eukaryotic algae during Snowball Earth events.

2. Penetration of Sea Glaciers

Campbell et al. [2011] used an analytical solution of momentum balance and continuity equations to calculate the distance that an incoming sea glacier would advance up the channel, referred to as penetration length. That analytical model assumed a uniform channel width. The mean-annual surface temperature and sublimation rate were independently specified, both were spatially uniform and constant in time. That model included only lateral shear stresses and assumed no longitudinal stretching; those conditions ensured a linear thickness gradient in the downstream direction and no thickness gradient in the lateral direction. Penetration length was determined to be a function of upstream ice thickness, channel width, ice softness (which is controlled by the mean-annual surface temperature), and sublimation rate. *Campbell et al*. [2011] did not address the effect of melting at the lower surface of the sea glacier. When the model was applied to a channel with the same mean length and mean width as the Red Sea (a modern analogue, because continental rifting, which is responsible for the Red Sea, would have been active during the Neoproterozoic), a restrictive range of surface temperatures and net sublimation rates allow the Red Sea to remain free of sea-glacier penetration. *Campbell et al*. [2011] concluded with a suggestion that a narrow entrance to the channel, a feature observed in the modern Red Sea, would decrease the penetration length of an incoming sea glacier by restricting the flow of ice into the channel, expanding the possible range of conditions that would allow the channel to be partially free from sea-glacier penetration. *Campbell et al*. [2011] contained an error in its calculations of sea-glacier penetration, which is corrected in Appendix A of this paper.

3. Model

Previously, we developed an analytical model to calculate sea-glacier penetration length L into a narrow channel [*Campbell et al*., 2011] with uniform width. That solution is limited in applicability because it calculates only the lateral shearing stress component and assumes a uniform lateral ice thickness and a linear downstream thickness profile. That model is not applicable to a channel with a varying width.

Here we develop a numerical model that resolves both lateral shearing and longitudinal stretching. This new model allows for a freely developing thickness field and is able to simulate the effect of a narrow entrance. In this new model, we couple equations of motion based on the Shallow Shelf Approximation to a time-independent mass conservation equation. We specify mean-annual surface temperature and sublimation rate. Then a Glen's Flow Law viscosity is used with an ice softness parameter based on the mean-annual surface temperature. To determine penetration length L, we iteratively the change channel length until the dynamic ice flux entering the channel balances the kinematic ice flux lost by sublimation. These equations are solved using a commercially available finite element solver, COMSOL Multiphysics® (comsol.com).

3.1. Body Equations

We use equations of motion that describe the flow of a layer of floating ice with thickness h much less than horizontal extent, commonly called the Shallow Shelf Approximation (SSA) [*Morland*, 1987; *MacAyeal et al*., 1996]

AGU Journal of Geophysical Research: Oceans 10.1002/2013JC009703

$$\frac{\partial}{\partial x}\left(2\nu h\left(2\frac{\partial u}{\partial x}+\frac{\partial v}{\partial y}\right)\right)+\frac{\partial}{\partial y}\left(\nu h\left(\frac{\partial u}{\partial y}+\frac{\partial v}{\partial x}\right)\right)=\rho_i g h\frac{\partial S}{\partial x}, \tag{1}$$

$$\frac{\partial}{\partial x}\left(\nu h\left(\frac{\partial u}{\partial y}+\frac{\partial v}{\partial x}\right)\right)+\frac{\partial}{\partial y}\left(2\nu h\left(\frac{\partial u}{\partial x}+2\frac{\partial v}{\partial y}\right)\right)=\rho_i g h\frac{\partial S}{\partial y}, \tag{2}$$

where x and y represent the horizontal spatial coordinates, u and v represent the corresponding velocities, ν represents the viscosity, h represents the ice thickness, ρ_i represents the ice density, g represents the acceleration of gravity, and S represents the surface elevation above sea level. The SSA assumes the ice is in hydrostatic equilibrium (i.e., floating); therefore, surface elevation is related to local thickness by a buoyancy relation

$$S=\left(1-\frac{\rho_i}{\rho_w}\right)h, \tag{3}$$

where ρ_w represents the water density.

Coupled to the SSA is a time-independent mass conservation equation

$$\nabla\cdot(\vec{u}h)+\dot{b}=0, \tag{4}$$

where $\dot{b}$ represents the net sublimation rate and $\vec{u}$ represents the velocity vector.

An effective viscosity is used that embodies Glen's Flow Law [*Glen*, 1955]

$$\nu=\frac{A^{-1/n}}{2}\left[\left(\frac{\partial u}{\partial x}\right)^2+\left(\frac{\partial v}{\partial y}\right)^2+\frac{1}{4}\left(\frac{\partial u}{\partial y}+\frac{\partial v}{\partial x}\right)^2+\left(\frac{\partial u}{\partial x}\frac{\partial v}{\partial y}\right)\right]^{\frac{1-n}{2n}}, \tag{5}$$

where n represents a flow rate exponent and A represents a temperature dependent softness parameter (described below in section 3.4).

3.2. Boundary Conditions

To solve the equations of motion and the mass conservation equation, boundary conditions must be imposed. There are three types of boundaries considered in this 2-D model: the entrance, the sidewalls, and the sea-glacier front. At the entrance, ice moves into the channel from the global sea glacier. To represent the entrance boundary condition, a uniform thickness H_0 is maintained along the entrance boundary. Ice is frozen stuck to the sidewalls. To represent the sidewalls, a no-slip boundary condition $(\vec{u}=\vec{0})$ is imposed. At the sea-glacier front, ice contacts seawater where it is in hydrostatic equilibrium

$$\int_{-\frac{\rho_i}{\rho_w}h}^{(1-\frac{\rho_i}{\rho_w})h}\bar{T}\cdot\vec{n}\,dz=-\frac{\rho_w g}{2}\left(\frac{\rho_i}{\rho_w}h\right)^2\vec{n}, \tag{6}$$

where $\bar{T}$ represents the stress tensor, and $\vec{n}$ represents an outward pointing normal vector.

3.3. Modifications

To solve the SSA, ice thickness h must be positive throughout the entire model domain, so we specify a small minimum thickness h_{min}. To enforce this condition, the SSA, sea-glacier front boundary condition, and the continuity condition are modified. If a particular point in the model has a thickness less than h_{min}, the SSA and sea-glacier front boundary condition use h_{min} in place of h. The continuity equation is modified so that if a particular node has thickness less than h_{min}, it will adjust the thickness to be h_{min} on the next iteration. The penetration length shows very little dependence on the choice of h_{min} in the range from 5 to 50 m.

The continuity equation is further modified to allow for artificial diffusion to avoid numerical instability. A set of representative experiments shows that neither of these modifications significantly affects the final solution. In these experiments, we first achieve a stable sea-glacier model using the above method; then a

AGU Journal of Geophysical Research: Oceans 10.1002/2013JC009703

Table 1. Constants Used in Analysis

Name	Symbol	Value	Units
Temperature-independent ice softness coefficient	A_0	4×10^{-13}	$Pa^{-3}\ s^{-1}$
Upstream ice thickness	H_0	650	m
Minimum ice thickness	h_{min}	20	m
Clausius-Clapeyron exponent	G	51	kJ/mol
Acceleration of gravity	g	9.81	m/s^2
Flow law exponent	n	3	Dimensionless
Activation energy for creep	Q_c	60	kJ/mol
Ideal gas constant	R	8.314	$J\ mol^{-1}\ K^{-1}$
Main channel width	W	200	km
Thermal diffusivity of ice	κ	1.2×10^{-6}	m^2/s
Ice density	ρ_i	917	kg/m^3
Seawater density	ρ_w	1043	kg/m^3

new model without these modifications is initialized with the solution from our stable solution. These models do achieve stability, without significant changes to the velocity and thickness fields.

3.4. Model Parameters

Values of the parameters used in the model are summarized in Table 1. Upstream ice thickness H_0 is chosen to be 650 m, based on equatorial ice-thickness model results from *Goodman* [2006]. Channel width W of 200 km is chosen to be similar to the modern Red Sea. Basal temperatures were calculated by adjusting the melting point of ice for pressure and salt content. Salt content was estimated by assuming present-day total salinity and total volume of the ocean, and adjusting the salinity taking into account the salt-free ice covering the ocean during a Snowball Earth event; this gives a salinity about 20% greater than modern, and a freezing temperature of $-2.3°C$, instead of $-1.9°C$. A relationship between the ice temperature and the softness parameter $A(T)$ has been derived empirically [*Cuffey and Paterson*, 2010, p. 75] and has a functional form

$$A(T) = A_0\, exp\left(\frac{-Q_c}{RT}\right), \tag{7}$$

where A_0 represents a temperature-independent softness coefficient, Q_c represents the activation energy for creep, R represents the ideal gas constant, and T represents the ice temperature in Kelvin. Because the rate of vertical advection of heat is small compared to the heat conduction rate, we assume a linear temperature profile throughout the ice thickness. Then we calculate an effective isothermal ice softness parameter A that satisfies force balance and produces the same ice flux in the channel as the value obtained by using the nonuniform temperature profile; a full explanation is given in *Campbell et al.* [2011, supporting information]. This new isothermal ice softness parameter A is used in place of the depth-dependent A in all equations that follow. This approximation allows us to use the SSA.

3.5. Solution Scheme

A rectangular model domain is used to represent the inland sea, with a channel width W and an adjustable channel length L. The geometry uses a mesh with triangular elements. The model is iterated upon until consistent fields of velocity, thickness, and viscosity are obtained. A dynamic flux is calculated by integrating ice flow across the entrance. A kinematic flux is calculated by integrating sublimation over the upper surface of the sea glacier. Channel length is adjusted by a root-finding scheme until the dynamic flux balances the kinematic flux, at which point we declare the channel length to be the penetration length of the sea glacier.

4. Experiments

We report on two sets of experiments: a validation experiment and a test of the effect of a narrow entrance.

4.1. Comparison to Analytical Model

We apply the numerical model to the idealized geometry used in the analytical model [*Campbell et al.*, 2011], for the same range of surface temperatures and sublimation rates (Figure 2). Penetration lengths

AGU Journal of Geophysical Research: Oceans 10.1002/2013JC009703

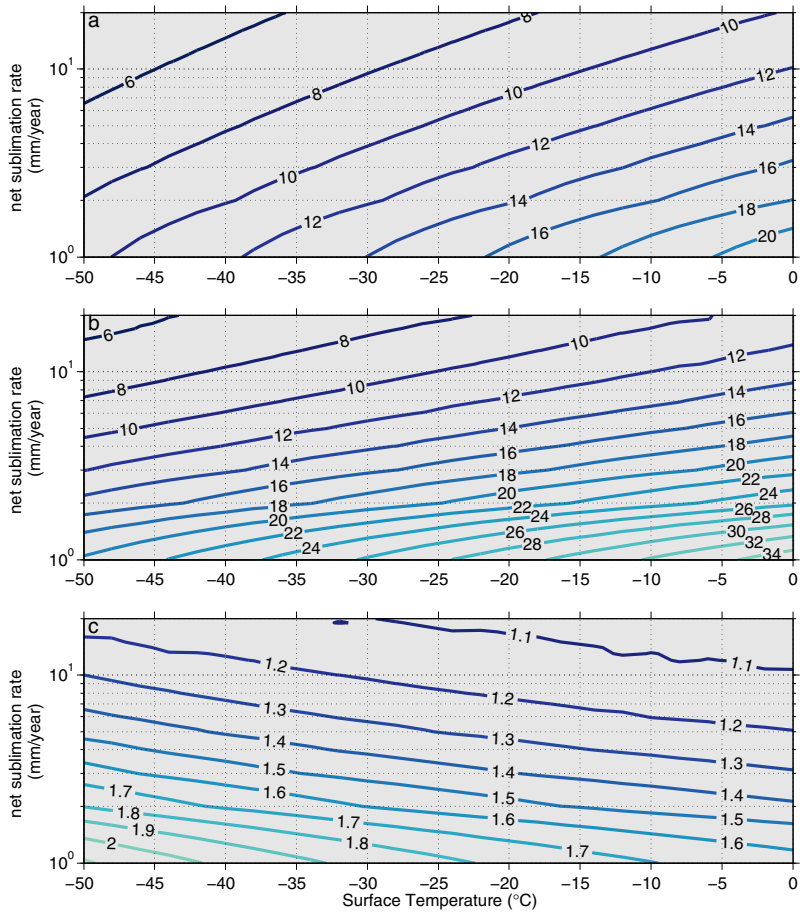

Figure 2. Contours represent the ratio of penetration length to channel width L/W as a function of net sublimation rate $\dot{b}$ (mm of ice equivalent per year)and surface ice temperature T_s for a sea glacier with an initial thickness $H_0 = 650$ m, entering an inland sea. (a) Results from the corrected analytical solution of *Campbell et al.* [2011] (see Appendix A of this work). (b) Results from Shallow Shelf Approximation numerical model developed here. (c) Ratio of the numerical model's L/W to the analytical model's L/W.

calculated by the numerical model are larger than those of the analytical solution, by up to a factor of 2, particularly at low net sublimation rates. The effect is diminished at larger sublimation rates, with at most a 30% increase in penetration length at net sublimation rates above 10 mm/yr.

4.2. Narrow Entrance Experiment

To determine the effect of a narrow entrance, we allow the width of the entrance to change while the width of the main channel remains constant. For this experiment, the boundaries adjacent to the entrance are treated as sidewalls. We calculate penetration length over the same range of mean-annual surface temperature and sublimation rate as in Figure 2 and in addition we vary the ratio of entrance width to channel width, W_s/W, from 5% to 100%. An example calculation of penetration length to channel width ratio L/W is shown in Figure 3a for W_s/W of 30%. In *Campbell et al.* [2011], we used the Red Sea as an analogue for the type of inland seas we expect to have existed during Snowball Earth events. The L/W of the Red Sea is 6.5, but other inland seas have differing L/W. The choice of $L/W = 6.5$ as a cutoff is simply a baseline for comparison. A refugium is possible only for combinations of T_s and $\dot{b}$ above the dashed line. Figure 3b tracks the 6.5 L/W contour as a function of W_s/W, showing that the range of climates permitting a refugium expands

AGU Journal of Geophysical Research: Oceans 10.1002/2013JC009703

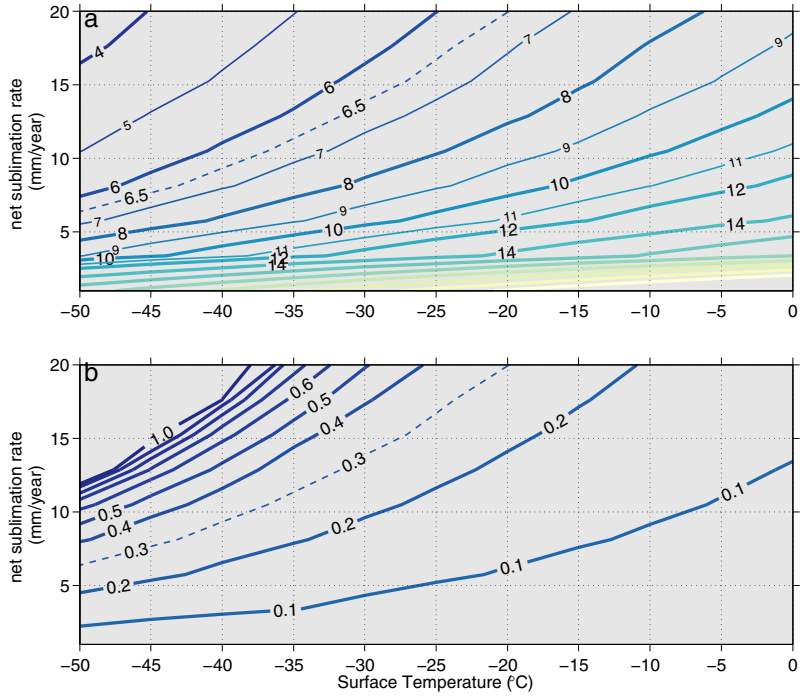

Figure 3. (a) Solid contours represent penetration length-to-width ratio L/W as a function of net sublimation rate $\dot{b}$ and surface ice temperature T_s for a sea glacier with an entrance width of 0.3 times the channel width. (b) The $L/W = 6.5$ contour, representative of the Red Sea, is tracked as a function of ratio of entrance width to channel width W_s/W with solid contours. The dashed contours in each part are the same contour with $L/W = 6.5$ and $W_s/W = 0.3$.

as the entrance narrows. Figure 4a shows the thickness and velocity fields for a sea glacier entering a channel where $T_s = -50°C$, $\dot{b} = 18$ mm/yr, and $W_s/W = 0.125$.

5. Thermal Evolution of an Invading Sea Glacier

In order for an inland sea to act as a refugium the atmospheric temperature must be warm enough that thick sea ice will not grow locally. The far end of the inland sea must therefore not be much below the melting temperature of ice. This situation is plausible because the oasis at the end of the channel would be surrounded by unglaciated desert land with albedo much lower than that of the ice-covered ocean.

As a cold sea glacier begins to invade into a warm inland sea, the sea glacier will warm, softening the ice. This effect will accelerate the sea glacier causing it to penetrate farther into the inland sea. However, as an inland sea goes from a cold temperature near its entrance, toward a warmer region, the associated net sublimation rate will increase. This effect reduces the penetration length of the sea glacier into the inland sea. The effects of increasing ice softness and increasing net sublimation are therefore in competition in determining sea-glacier penetration. In this section, we couple a thermal evolution model to the ice-flow model to determine whether the combination of these effects reduces or increases sea-glacier penetration.

5.1. Dependence of Net Sublimation Rate on Temperature

Atmospheric temperature varies over the inland sea; the ice surface temperature, and the net sublimation rate will vary correspondingly. Here we prescribe the surface temperature field and calculate the associated net sublimation rate. At the upstream end of the inland sea we choose an initial surface temperature T_{s0} to

AGU Journal of Geophysical Research: Oceans 10.1002/2013JC009703

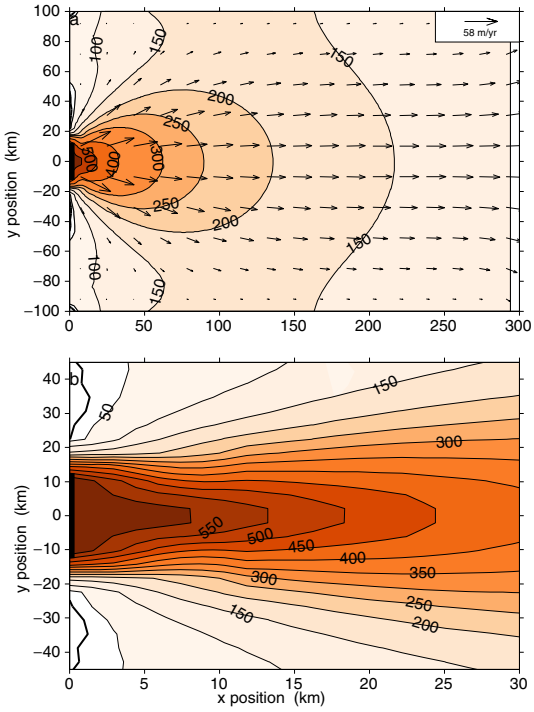

Figure 4. Results for a sample sea-glacier penetration model where the surface temperature $T_s = -50°C$, the net sublimation rate $\dot{b} = 18$ mm /yr, and the ratio of entrance width to channel width $W_s/W = 0.125$. Thin contours represent the ice thickness h in meters. Arrows indicate flow rate and direction; a reference arrow is in the upper right portion of this figure. The thick bar centered at $y = 0$ represents the channel entrance. The thick contours adjacent to the entrance represent areas where $h \leq h_{min}$, which we interpret as ice-free zones. The contour interval is 50 m. (a) The entire model domain. (b) An enlarged section near the entrance. Note the differing aspect ratios between (a) and (b).

be the equatorial surface temperature of the global sea glacier, with corresponding sublimation rate $\dot{b}_0$. We linearly vary the atmospheric temperature along the downstream direction of the sea glacier (the x direction, with $x = 0$ at the entrance), assuming the temperature is uniform across the width of the channel (the y direction),

$$T_s(x,y) = T_{s0} + \frac{(T_m - T_{s0})x}{L_t}, \quad (8)$$

where L_t represents the transition distance for the inland sea to reach $T_m = 273$ K. Here we assume that changes in $\dot{b}$ are proportional to changes in the saturation vapor pressure according to the Clausius-Clapeyron relation

$$\dot{b}(T_s) = c\, exp\left(\frac{-G}{RT_s}\right), \quad (9)$$

where c represents a constant which gives $\dot{b}(T_{s0}) = \dot{b}_0$, and G represents the Clausius-Clapeyron exponent from *Marti and Mauersberger* [1993].

5.2. Thermal Evolution Model

To calculate the thermal evolution of a penetrating sea glacier, we couple a 1-D thermal diffusion and vertical advection model to the previously described ice-flow model. Using the centerline velocity, we are able to track a column of ice as it advects downstream over time, and to calculate the centerline temperature profile.

We use a 1-D thermal diffusion and vertical advection model following *Hooke* [2005]

$$\frac{\partial T}{\partial t} = \kappa \frac{\partial^2 T}{\partial z^2} - w\frac{\partial T}{\partial z}, \quad (10)$$

where t represents the time, κ represents the thermal diffusivity of ice, z represents a positive-upward vertical coordinate, and w represents the corresponding vertical velocity. Vertical velocity is assumed to go linearly to zero at the base of the sea glacier:

$$w = \frac{z}{h} w_s, \quad (11)$$

where w_s represents the vertical velocity at the surface of the glacier. For this calculation, z is set to be zero at the local sea-glacier base and vertical velocity at the surface w_s is calculated to balance the sublimation rate and the depth-averaged strain rate:

AGU Journal of Geophysical Research: Oceans 10.1002/2013JC009703

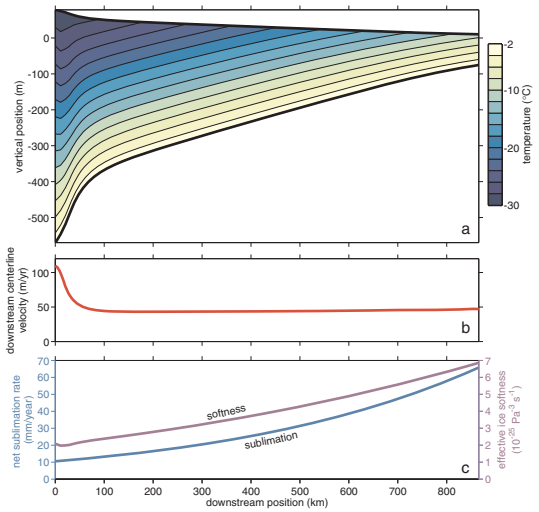

Figure 5. Results for the thermal evolution model for the centerline of an invading sea glacier. For this example $T_{s0} = -30°C$, $\dot{b}_0 = 10.5$ mm/yr, and $W_s/W = 0.3$. (a) Contours represent the ice temperature. (b) The downstream component of velocity. (c) Effective ice softness A and sublimation rate $\dot{b}$.

$$w_s = -\dot{b} - \left(\frac{\partial u}{\partial x} + \frac{\partial v}{\partial y}\right) h. \quad (12)$$

The model is forced by temperature boundary conditions of T_s at the upper surface and the pressure-dependent melting temperature (see section 3.4) at the basal surface. We choose an upper-surface temperature T_{s0} and net sublimation rate $\dot{b}_0$ at the entrance based on the ranges provided in Figure 2.

5.2.1. Model Coupling

The thermal evolution model generates a centerline temperature profile. For every x position, we calculate an integrated ice softness A (see section 3.4) and we assume it is laterally (y direction) uniform. We then use these ice softnesses and their associated net sublimation rates in the ice-flow model described in section 3. With a new centerline velocity, we iteratively feed results back and forth between the thermal model and the ice-flow model until a stable solution is reached.

5.3. Results of Thermal Model

Figure 5a shows the temperature profile for an invading sea glacier with $T_{s0} = -30°C$, $\dot{b}_0 = 10.5$ mm/yr, and W_s/W of 30%. The values of T_{s0} and $\dot{b}_0$ are consistent with climatic conditions expected for the equator of Snowball Earth [*Pierrehumbert et al.*, 2011]. Figure 5c shows that in a warming channel, the ice softness A increases more slowly than the net sublimation rate $\dot{b}$. Thus, the penetration length of the sea glacier is reduced in comparison to a channel with uniform surface temperature and sublimation rate. Although this is a specific example, the pattern of diminished sea-glacier penetration is true for all combinations of T_s, $\dot{b}$, and W_s explored in this work.

6. Discussion

6.1. Sea-Glacier-Free Zones

In order to solve the SSA, a small, positive minimum ice thickness h_{min} must be enforced throughout the model domain. The minimum ice thickness chosen here is of the same order of magnitude as the greatest ice thickness that allows for photosynthesis to occur underneath bubble-free ice [*Warren et al.*, 2002]. Therefore, sea-glacier-free zones may have acted as refugia, provided that thick sea ice did not grow locally.

In all experiments, ice thickness diminished to h_{min} at the downstream end after traveling a sufficient distance. The narrow-entrance experiment also revealed areas adjacent to the entrance where ice thickness reached h_{min} (Figure 4). Ice enters the channel through a narrow entrance and is forced to flow laterally and, at some locations, backward to flow into areas adjacent to the entrance. In the example shown in Figure 4, there are areas 20–40 km away from the channel entrance where $h = h_{min}$. In the model, there are "sea-glacier-free" regions because we artificially prevented $h < h_{min}$, so we interpret these areas to be completely free of sea-glacier ice. We had anticipated that sea-glacier-free areas could exist only far downstream of the channel entrance; however, for a channel with a narrow entrance, it is possible to have ice-free areas located near the entrance on the upstream end of the channel. Not all experiments produced sea-glacier-free zones near the entrance; they were found primarily in experiments with narrow entrances, high net

AGU Journal of Geophysical Research: Oceans 10.1002/2013JC009703

sublimation, and low surface temperature. In fact, the net sublimation rate specified for Figure 4 (10.5 mm/yr) is probably larger than would occur for the specified $T_s = -50^{\circ}$C.

Sea-glacier-free zones near the channel entrance would grow thick ice locally if they are located in a cold region of the inland sea. We conclude that none of the sea-glacier-free zones observed in our models near the channel entrance would act as refugia, because they are only observed with colder temperatures that would locally generate thick sea-ice.

The discovery that sea-glacier-free zones can be located away from the downstream end of a channel indicates that our assumption of a rectangular channel might limit our ability to discover and categorize other ice-free areas that are possible for ice entering a narrow channel. Natural channels are not perfectly rectangular. It is possible that shallow spots and side channels could generate ice shadows and ice-free areas that are not located at the downstream end of a single main channel. Obstructions upstream from the terminus, but where atmospheric temperatures are warm enough, may generate sea-glacier-free zones that could act as refugia.

6.2. Submarine Melting

Submarine melting is not explicitly taken into account in this study. However, the presence of submarine melting or freezing could be accounted for in this model by adjusting the net sublimation rate $\dot{b}$ in the continuity equation (equation (4)). *Ashkenazy et al*. [2013] have used a coupled ocean-atmosphere GCM to calculate both surface net sublimation and submarine melting for a Snowball Earth scenario. That study found that regions with net sublimation also experience a similar magnitude of submarine melt. The special environment of an inland sea may inhibit that process; inland seas are restricted waterways with thick ice that would partially block the underwater channel entrance. However, rift-valley seas can experience enhanced geothermal flux which could thin the ice. Since we do not know whether inland seas in a net-sublimation region would experience net melting or net freezing, we choose to not address that effect in this work.

6.3. Atmospheric Constraints

While we can now determine the penetration of a sea glacier into a narrow channel with a narrower entrance for a given mean-annual surface temperature and net sublimation rate, we have not assessed the likelihood of an inland sea to possess those climate conditions. Robust elements of Snowball climate have been determined [*Abbot et al*., 2013]; however, the climate of an inland sea is a special environment that has not been considered in the previous studies. The inland sea environment is a channel surrounded by land with a sea glacier at the entrance. The only place where a sea glacier cannot penetrate a channel is in a region of net sublimation, which, according to GCM results for Snowball Earth are mostly near the equator [*Pierrehumbert et al*., 2011; *Pollard and Kasting*, 2004, Figure 9]. Since inland seas are allowed only in regions of net sublimation, any land areas surrounding the inland sea would likely be desert, covered with bare rock or soil, not snow or ice, although others have indicated that some or all of the land in regions of net sublimation could become covered with land ice flowing from regions of net accumulation [*Donnadieu et al*., 2003; *Pollard and Kasting*, 2004; *Rodehacke et al*., 2013]. If it is unglaciated, the low albedo of the rock and soil surrounding the inland sea would increase absorbed radiation and locally increase the air temperature. If an inland sea is mostly surrounded by bare land, the air temperature and sublimation rate would therefore be greater than on a sea glacier over ocean at the same latitude. The albedo of modern deserts is 0.3–0.4 [*Smith*, 1986; *Otterman and Fraser*, 1976] much lower than our estimate for that of a sublimating sea glacier, ~0.6 [*Dadic et al*., 2013]. To fully evaluate the likelihood of regional temperatures sufficiently warm to sustain an oasis will require investigation with a general circulation model.

6.4. Grounding of the Sea Glacier

An assumption of *Campbell et al*. [2011] is that the channel is deep enough so the penetrating sea glacier never runs aground (i.e., the sea glacier is always floating). If the Red Sea is again chosen as a suitable analogue, this condition does not hold. The penetrating sea glacier could have an initial thickness as small as 600 m, based on modeling of a water-planet sea-glacier [*Goodman*, 2006], but the entrance to the Red Sea is only 137 m deep [*Siddall et al*., 2002]. Clearly, the assumption that the sea glacier is always floating cannot be true everywhere in the channel. This problem can be addressed with by a modification of the ice-shelf equations in *Morland* [1987] as *MacAyeal* [1989] has done, or by using a fully 3-D ice-flow model treating grounding-line dynamics.

AGU Journal of Geophysical Research: Oceans 10.1002/2013JC009703

7. Conclusions

In this work, we tested the ability a sea glacier to penetrate an inland sea with a narrow entrance. We discovered that by reducing the size of the channel entrance, sea-glacier penetration becomes more limited. A sea glacier entering into an inland sea with a warming atmospheric temperature will not penetrate as far into a channel as compared to a channel with uniform atmospheric temperature and sublimation rate. We also discovered that sea-glacier-free zones might exist near the entrances of some channels with narrow entrances, but would not act as refugia at the cold temperatures near the entrance. These results widen the range of climate conditions that allow for inland seas to act as refugia for photosynthetic eukaryotic algae during Snowball Earth events.

Appendix A: Correction to *Campbell et al.* [2011]

There are two errors in *Campbell et al.* [2011] that we wish to correct. The cumulative effect of these corrections is that penetrations lengths are approximately 70% greater than reported in our original Figure 2. The first correction was made because of a plotting error in Figure 2 of our paper, hereafter referred to as C2011. This correction made the penetration lengths shown in Figure 2 of C2011 increase by approximately 40%.

The second correction was made because the ice velocities predicted by equation (2) of C2011 are all too small by a factor of 2. This correction caused an increase in penetration length of approximately 20%, affecting both Figures 2 and 3b of C2011. The correction was needed because *Nye*'s [1965] definition of a temperature-dependent ice-softness $A(T)$ parameter differed by a factor of 2 from the definition of $A(T)$ in current standard usage [e.g., *Cuffey and Paterson*, 2010, p. 75]. This difference corresponds to a difference of about 6 K in ice temperature T. The correct form of equation (2) of C2011 is

$$u(x,y)=W\frac{A(x)k(x)^n}{n+1}\left(1-\left|\frac{2y}{W}\right|^{n+1}\right). \tag{A1}$$

This correction affects some equations from C2011 that follow. The right sides of equations (3), (15), (S-14), (S-15), the two rightmost expressions of equation (S-19), and the left sides of equations (6) and (9) are all too small by a factor of 2, and because of a nonlinear constitutive relationship for ice, equation (14) should have the form

$$D=\left(\frac{2^n\dot{b}(n+2)}{A\Gamma^n}\right)^{\frac{1}{n+1}}. \tag{A2}$$

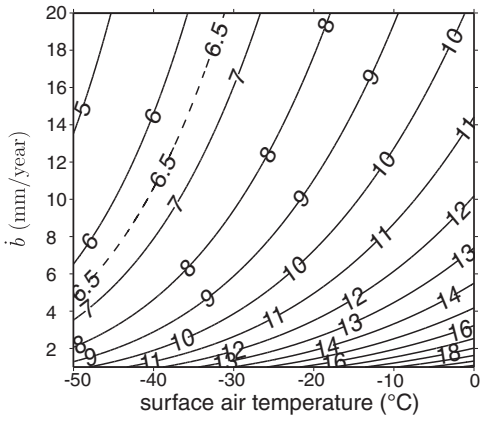

Figure 6. Solid contours represent the penetration length-to-width ratio L/W as a function of net sublimation rate $\dot{b}$ and surface ice temperature T_s for a sea glacier with an initial thickness $H_0 = 650$ m, entering a narrow channel. Dashed line represents the 6.5 L/W ratio for the Red Sea. Atmospheric conditions to the left of the dashed line allow a refugium to avoid being over-ridden at the end of the Red Sea analogue.

A corrected Figure 2 of C2011 appears here as Figure 6. The penetration length was increased by approximately 70%, further restricting the climatic conditions for which a refugium is allowed. A corrected Figure 3 of C2011 appears here as Figure 7. The bounds for Figure 7b were changed, but the overall shape remains unchanged. [Figure 7a is identical to the published figure.] As modeled here, an analogue to the Red Sea is long enough to have provided a refugium for photosynthetic organisms during Snowball Earth events, only if surface temperature and net sublimation conditions in Figure 6 were met, for example, a −40°C mean-annual surface temperature with a 10 mm/yr net sublimation rate, which seems unlikely.

Journal of Geophysical Research: Oceans 10.1002/2013JC009703

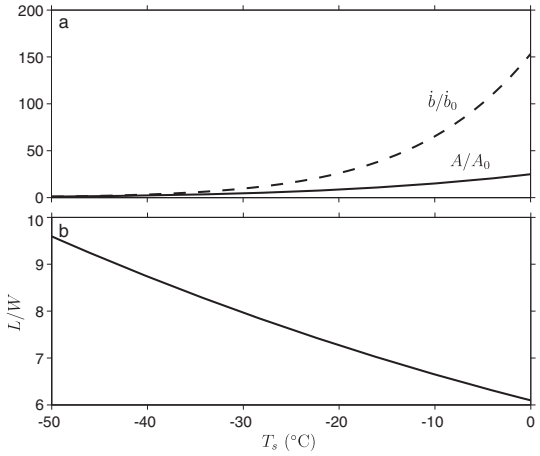

Figure 7. Top plot (a) shows how increasing atmospheric temperatures during deglaciation affect net sublimation rate $\dot{b}$, relative to an initial value $\dot{b}_0$ of 1 mm/yr (dashed line), and ice softness A, relative to an initial value A_0 set by a surface temperature $T_s = -50°C$ (solid line). Net sublimation rate $\dot{b}$ is more sensitive than ice softness A to rising surface temperature T_s. Bottom plot (b) shows resulting length-to-width ratio L/W of a invading sea glacier, calculated from equation (13). For this particular example, the initial upstream ice thickness is $H_0 = 650$ m.

Acknowledgments
We thank Olga Sergienko for assistance with the numerical ice flow modeling and T.J. Fudge for assistance with the thermal evolution model. We thank Dorian Abbot and an anonymous reviewer for their thoughtful reading that improved the content and presentation of this article. This work is supported by NSF grant ANT-11–42963.

References

Abbot, D. S., A. Voigt, D. Li, G. Le Hir, R. T. Pierrehumbert, M. Branson, D. Pollard, and D. D. B. Koll (2013), Robust elements of Snowball Earth atmospheric circulation and oases for life, *J. Geophys. Res.*, *118*, 6017–6027, doi:10.1002/jgrd.50540.

Ashkenazy, Y., H. Gildor, M. Losch, F. A. Macdonald, D. P. Schrag, and E. Tziperman (2013), Dynamics of a Snowball Earth ocean, *Nature*, *495*(7439), 90–93, doi:10.1038/nature11894.

Campbell, A. J., E. D. Waddington, and S. G. Warren (2011), Refugium for surface life on Snowball Earth in a nearly-enclosed sea? A first simple model for sea-glacier invasion, *Geophys. Res. Lett.*, *38*, L19502, doi:10.1029/2011GL048846.

Cuffey, K. M., and W. S. B. Paterson (2010), *The Physics of Glaciers*, 4th ed., 693 pp., Elsevier, Amsterdam.

Dadic, R., P. C. Mullen, M. Schneebeli, R. E. Brandt, and S. G. Warren (2013), Effects of bubbles, cracks, and volcanic tephra on the spectral albedo of bare ice near the Trans-Antarctic Mountains: Implications for sea-glaciers on Snowball Earth, *J. Geophys. Res. Earth Surf.*, *118*, 1658–1676, doi:10.1002/jgrf.20098.

Donnadieu, Y., F. Fluteau, G. Ramstein, C. Ritz, and J. Besse (2003), Is there a conflict between the Neoproterozoic glacial deposits and the snowball Earth interpretation: An improved understanding with numerical modeling, *Earth Planet. Sci. Lett.*, *208*(1–2), 101–112.

Glen, J. W. (1955), The creep of polycrystalline ice, *Proc. R. Soc. London, Ser. A*, *228*(1175), 519–538, doi:10.1098/rspa.1955.0066.

Goodman, J. C. (2006), Through thick and thin: Marine and meteoric ice in a Snowball Earth climate, *Geophys. Res. Lett.*, *33*, L16701, doi:10.1029/2006GL026840.

Goodman, J. C., and R. T. Pierrehumbert (2003), Glacial flow of floating marine ice in Snowball Earth, *J. Geophys. Res.*, *108*(C10), 3308, doi:10.1029/2002JC001471.

Hoffman, P. F., and D. P. Schrag (2002), The snowball Earth hypothesis: Testing the limits of global change, *Terra Nova*, *14*(3), 129–155.

Hooke, R. L. (2005), *Principles of Glacier Mechanics*, 2nd ed., 429 pp., Cambridge Univ. Press, Cambridge, U. K.

Knoll, A. (1992), The early evolution of eukaryotes: A geological perspective, *Science*, *256*(5057), 622–627, doi:10.1126/science.1585174.

Li, D., and R. T. Pierrehumbert (2011), Sea glacier flow and dust transport on Snowball Earth, *Geophys. Res. Lett.*, *38*, L17501, doi:10.1029/2011GL048991.

MacAyeal, D. R. (1989), Large-scale ice flow over a viscous basal sediment: Theory and application to ice stream B, Antarctica, *J. Geophys. Res.*, *94*(B4), 4071–4087.

MacAyeal, D. R., V. Rommelaraere, P. Huybrechts, C. L. Hulbe, J. Determann, and C. Ritz (1996), An ice-shelf model test based on the Ross Ice Shelf, Antarctica, *Ann. Glaciol.*, *23*, 46–51.

Macdonald, F. A., M. D. Schmitz, J. L. Crowley, C. F. Roots, D. S. Jones, A. C. Maloof, J. V. Strauss, P. A. Cohen, D. T. Johnston, and D. P. Schrag (2010), Calibrating the Cryogenian, *Science*, *327*(5970), 1241–1243, doi:10.1126/science.1183325.

Marti, J., and K. Mauersberger (1993), A survey and new measurements of ice vapor pressure at temperatures between 170 and 250 K, *Geophys. Res. Lett.*, *20*(5), 363–366.

Morland, L. (1987), Unconfined ice-shelf flow, in *Dynamics of the West Antarctic Ice Sheet*, edited by C. J. van der Veen and J. Oerlemans, pp. 99–116, Kluwer Acad., Dordrecht, Netherlands.

Nye, J. F. (1965), The flow of a glacier in a channel of rectangular, elliptical or parabolic cross-section, *J. Glaciol.*, *5*(41), 661–690.

Otterman, J., and R.S. Fraser (1976), Earth-atmosphere system and surface reflectivities in arid regions from Landsat MSS data, *Remote Sens. Environ.*, *5*, 247–266.

Pierrehumbert, R. T., D. S. Abbot, A. Voigt, and D. Koll (2011), Climate of the Neoproterozoic, *Annu. Rev. Earth Planet. Sci.*, *39*(1), 417–460, doi:10.1146/annurev-earth-040809-152447.

AGU Journal of Geophysical Research: Oceans 10.1002/2013JC009703

Pollard, D., and J. F. Kasting (2004), Climate-ice sheet simulations of Neoproterozoic glaciation before and after collapse to Snowball Earth, in *The Extreme Proterozoic: Geology, Geochemistry, and Climate, Geophys. Monogr. Ser.*, vol. 146, edited by G. S. Jenkins et al., pp. 91–105, AGU, Washington, D. C.

Rodehacke, C. B., A. Voigt, F. Zieman, and D. S. Abbot (2013), An open ocean region in Neoproterozoic glaciations would have to be narrow to allow equatorial ice sheets, *Geophys. Res. Lett.*, *40*, 5503–5507, doi:10.1002/2013GL057582.

Siddall, M., D. A. Smeed, S. Matthiesen, and E. J. Rohling (2002), Modelling the seasonal cycle of the exchange flow in Bab El Mandab (Red Sea), *Deep Sea Res., Part I*, *49*(9), 1551–1569, doi:10.1016/S0967-0637(02)00043-2.

Smith, E. A. (1986), The structure of the Arabian heat low, Part I: Surface energy budget, *Mon. Weather Rev.*, *114*, 1067–1083.

Tziperman, E., D. S. Abbot, Y. Ashkenazy, H. Gildor, D. Pollard, C. G. Schoof, and D. P. Schrag (2012), Continental constriction and sea ice thickness in a Snowball-Earth scenario, *J. Geophys. Res.*, *117*, C05016, doi:10.1029/2011JC007730.

Warren, S. G., R. E. Brandt, T. C. Grenfell, and C. P. McKay (2002), Snowball Earth: Ice thickness on the tropical ocean, *J. Geophys. Res.*, *107*(C10), 3167, doi:10.1029/2001JC001123.

Chapter 5

CAN PROMONTORIES RESTRICT SEA-GLACIER PENETRATION INTO MARINE EMBAYMENTS DURING SNOWBALL EARTH EVENTS?

In preparation for Earth and Planetary Science Letters

This third paper considers the effects of introducing promontories into the channels that sea glaciers invade. Inspired by the discovery of thin-ice zones in our previous work, we were curious to find out if promontories could create thin-ice zones on their downstream ends. Ice thinning as it flows around obstructions can be seen on the modern Earth. By applying the ice-flow model previously developed, we were able to calculate sea-glacier penetration into channels with promontories. We discovered the addition of a promontory restricts sea-glacier penetration, however, we were not able to conclusively demonstrate that true ice-free zones, necessary for refugia, could be formed on the downstream side of promontories. This remains a potential direction for future work.

For this work, I developed the solution for ice-flow model. B. Massarano modified the ice-flow model to introduce a promontory and performed the experiments. E. D. Waddington provided support for ice-flow modeling. S. G. Warren helped provide much of the background context of Snowball Earth.

Can promontories restrict sea-glacier penetration into marine embayments during Snowball Earth events?

Adam J. Campbell[1], Betzalel Massarano[1,2], Edwin D. Waddington[1], Stephen G. Warren[1,3]

[1] Department of Earth and Space Sciences, University of Washington, Seattle, Washington, USA

[2] now at Pacific Science Center, Seattle, Washington, USA

[3] Astrobiology Program, University of Washington, Seattle, Washington, USA

June 5, 2015

Abstract

Photosynthetic eukaryotic algae may have survived during the Snowball Earth events of the Neoproterozoic in marine embayments hydrologically connected to the global ocean. Previous studies have shown that marine embayments with straight shorelines could have acted as refugia, provided that climate and entrance geometries were suitable to prevent full penetration by thick sea glaciers. Here we test whether promontories, i.e. headlands emerging from a side shoreline, could restrict sea-glacier flow sufficiently to allow refugia under a broader range of climate conditions. We use an ice-flow model, suitable for floating ice, to demonstrate that promontories can expand conditions allowing refugia in two ways: 1) promontories can restrict the flow of invading sea glaciers, and expand the climate conditions that allow for refugia at the

21 downstream end of channels, and 2) promontories may generate sea-glacier-free zones, called
22 ice shadows, behind promontories of sufficient size.

23 1 Introduction

24 During the Neoproterozoic, the entire upper ocean surface may have been covered by ice
25 several hundreds of meters thick [*Goodman and Pierrehumbert*, 2003; *Goodman*, 2006; *Li and*
26 *Pierrehumbert*, 2011]. Ice covering the ocean, thick enough to deform under its own weight as
27 a "sea glacier," restricted the possible locations for survival of photosynthetic organisms. Fossil
28 evidence demonstrates that photosynthetic eukaryotic algae existed immediately prior to and
29 after these events [*Knoll*, 1992; *Macdonald et al.*, 2010], implying they survived during the
30 Snowball Earth events, but where these organisms survived is not clear.
31
32 Our previous studies considered the viability of marine embayments (referred as inland seas in
33 previous publications) to provide refugia for photosynthetic eukaryotes during the Snowball
34 Earth events of the Neoproterozoic [*Campbell et al.*, 2011, 2014]. We found that marine
35 embayments limit sea-glacier penetration and in regions of net sublimation the invading sea
36 glacier could be completely sublimated before reaching the end of the seaway. In the latter of
37 those studies, we considered ice flowing through a narrow entrance into a wider channel. Ice
38 that flows through a narrow entrance moves down channel, perpendicular to the entrance. After
39 some distance the ice spreads out laterally, slowly filling the regions immediately laterally
40 adjacent to the entrance [*Campbell et al.*, 2014; Figure 4]. We found that certain combinations
41 of entrance widths and climate conditions (i.e. temperature and sublimation rate) allowed for
42 sea-glacier-free regions to be located near the entrance of the channel. We hypothesized that a
43 similar situation could exist behind an obstruction (such as a promontory or island) farther along
44 the channel, creating a sea-glacier-free zone which we call an ice shadow, which might also be

free of locally-grown sea ice (Figure 1). We defined sea-glacier-free zones as regions where ice was too thin for our model to capture.

These ice shadows might provide refugia for photosynthetic organisms in channels that are otherwise completely penetrated by a sea glacier. Channels containing several ice-free spots would be more robust at preserving organisms during the glaciation-deglaciation cycle of a Snowball Earth event. Here we calculate the flow of floating ice around obstructions to address the questions: to what extent (if any) do promontories reduce sea-glacier penetration, and can promontories generate thin-ice-zones capable of acting as refugia?

In Section 2, we provide examples of modern ice shadows. Section 3 describes the methods we use for a sea-ice thickness calculation, ice flow modeling and experimental setup. In Section 4 we describe the results of our experiments. In Section 5 we discuss our results including how promontories affect sea-glacier penetration, and in Section 6 we summarize our conclusions.

2 Modern ice shadows

Features like ice shadows we are hypothesizing exist on the modern Earth. As floating ice approaches islands, promontories or other obstructions, the ice slows down and thickens. The overthickening creates a relatively steep surface gradient that allows ice to move faster as it flows around the obstruction. The fast flowing ice moving past the obstruction then has difficulty backflowing toward the downstream side of the obstruction, creating a thin-ice zone we refer to as an ice shadow. In McMurdo Sound, Antarctica, the Ross Ice Shelf creates an ice shadow as it flows past White Island (Figure 2a). On the far side of White Island the ice is thinned sufficiently to allow a tidal crack to remain nearly continuously open. In an interesting

69 coincidence, this ice shadow is a refugium. A colony of Weddell Seals remains isolated from
70 other Weddell Seal populations since an ice shelf advance that isolated White Island sometime
71 between 1947 and 1956, where the tidal crack remains their only point access from the land to
72 the ocean [*Gelatt et al.*, 2010]. An analogous situation in grounded ice is demonstrated by
73 Taylor Glacier in Antarctica, which flows past Finger Mountain (Figure 2b). A small distributary
74 of Taylor Glacier flows around Finger Mountain in a 180-degree turn, becoming the much-
75 thinner Turnabout Glacier, which then incompletely penetrates Turnabout Valley behind Finger
76 Mountain.

77 3 Methods

78 Here we explore how introducing a promontory into a channel affects ice flow. We calculate the
79 reduction of sea-glacier penetration and calculate the extent of ice-free area behind a region
80 behind a promontory. For a region behind a promontory to be an ice shadow suitable as a
81 refugium, two conditions must be met: the invading sea glacier must not penetrate the leeward
82 side of the promontory, and locally-grown sea ice must remain thin. To examine the conditions
83 for existence of such an ice shadow, we calculate (a) the ice thickness for locally-grown sea ice
84 and the atmospheric conditions needed for open water (Section 3.1), and (b) the flow of ice
85 around obstructions, for cases where those suitable atmospheric conditions have been met
86 (Section 3.3). These two requirements interact: warm surface temperature is needed to prevent
87 thick ice growing locally, but warm temperature softens glacier ice, allowing it to flow more
88 easily around corners.

89 3.1 Sea-glacier flow model

90 To simulate the behavior of a sea glacier flowing in a channel containing a promontory, we use
91 an ice flow model solving an approximation to the Navier-Stokes momentum balance equations

(called the Shallow Shelf Approximation) coupled to a time-independent mass conservation equation. Here we outline the ice-flow modeling procedure; interested readers can consult *Campbell et al.* [2014] for more details. The Shallow Shelf Approximation is an approximation of the Navier-Stokes equations that is suitable for floating ice where the vertical dimension is much smaller than the horizontal dimensions [*Morland*, 1987; *MacAyeal et al.*, 1996]. This model resolves both lateral shearing and longitudinal stretching. We specify mean-annual surface temperature and sublimation rate, both spatially uniform and temporally constant. A Glen's Flow Law viscosity is used [*Glen*, 1955] with an ice softness parameter based on the mean-annual surface temperature [*Cuffey and Paterson*, 2010, pg. 75]. To determine penetration length *L*, we iteratively change the channel length until the dynamic ice flux entering the channel balances the kinematic ice flux lost by sublimation. These equations are solved using a commercially available finite element solver, COMSOL Multiphysics® (comsol.com).

3.2 Sea-ice thickness calculation

Equilibrium sea ice thickness can be calculated by balancing a temperature-diffusion equation

$$h = \frac{k(T_f - T_s)}{\rho_i L_i \dot{b} + F_{geo}}, \quad (1)$$

where h represents the ice thickness, k the thermal conductivity, T_f the freezing temperature, T_s the surface temperature, ρ_i the density of ice, L_i the heat of fusion of ice, $\dot{b}$ the rate of ice growth at the base (assumed equal to the net sublimation rate in steady state), and F_{geo} the geothermal heat flux. The sublimation rate is linked to temperature by the Clausius-Clapeyron equation, as in *Campbell et al.* [2014]. Equation 1 is a simplification of Equation 1 of *Warren et al.* [2002] in which we have omitted the penetration of solar radiation. Equilibrium sea-ice thicknesses calculated using Equation 1 are shown in Figure 3. In this study, we are interested in combinations of surface temperature and sublimation rate that generate thin sea ice or open

116 water. For our purposes, we define thin sea ice to be less than or equal to 50 m, because that
117 is the model resolution for thin ice. By choosing not to consider the effect of solar absorption
118 within the ice, our sea-ice thickness calculations become an upper-bound for a given T_s and $\dot{b}$.
119 Values used to calculate *h* in Figure 3 are given in Table 1. The albedo of ice can strongly
120 affect sea-ice thickness with bare ice likely absorbing enough light to remain thin enough to
121 allow of photosynthesis under the ice surface [*Warren et al.*, 2002], however a salt crust may
122 develop on sea ice that would increase the sea-ice albedo [*Light et al.*, 2009],increasing ice
123 thickness and prohibiting photosynthesis under the ice surface.

124 3.3 Promontory experiments

125

126 To determine whether the extent an invading sea glacier penetrates the leeward side of the
127 promontory, we use the sea-glacier flow model described above in Section 3.1. We perform a
128 series of experiments to determine the amount of thinning as ice flows around a promontory.
129 The geometry of our experiments consists of an idealized rectangular channel with width *W* and
130 length *L*. A square promontory, with side-length L_p, is placed along one sidewall, centered at *x* =
131 0.85*L* (Figure 1). We make the assumption that the promontory walls and the channel side
132 walls are very steep and very high, and hence the sea glacier cannot move onto the
133 promontory; the case where a promontory is low and can be over-ridden by the sea glacier
134 would require a different model. We then solve iteratively for thickness *h*, penetration length L_g,
135 and the velocity field, while varying promontory size L_p and combinations of surface temperature
136 T_s and sublimation rate $\dot{b}$ along the 50 m ice-thickness contour (Figure 3) linearly varied from -
137 5.7°C to -4.6°C in 10 evenly-spaced increments. The promontory side length L_p is varied from 0
138 (i.e. no promontory) to 100km in 10 km increments.

139 We use two metrics to quantify the presence of downstream ice shadows: thickness drop and

critical percentage. Thickness drop $\Delta H \equiv \overline{H_U} - \overline{H_D}$ where $\overline{H_U}$ and $\overline{H_D}$ represent mean ice thickness in upstream and downstream regions respectively. Those upstream and downstream evaluation regions are chosen to have length $3L_p$ and width L_p and are located immediately upstream and downstream of the promontory (Figure 4a). Scaling the evaluation regions with the size of the promontory allows the thickness drop to be more completely captured than if we were to use evaluation regions of constant size. The spatial scale of the disturbance should scale with L_p. Critical percentage *CP* is defined as the percentage of the downstream evaluation region where ice thickness falls below a specified critical thickness value *CT*. Values of constants and boundary conditions used in the promontory experiments are given in .

4 Results

General patterns can be recognized from the ice flow modeling experiments. Ice thins as it flows around the promontory, slowing as it approaches the promontory and speeding up as it flows around it, as shown in a sample model (Figure 4) where T_s = -5.33 °C, $\dot{b}$ = 12.70 mm/yr, and L_p = 60 km. Far upstream of the promontory, velocity is slowest at the sidewalls and fastest directly between them. As the ice approaches the promontory, the fastest ice is located closer to the sidewall opposite the promontory and as the ice moves away from the promontory the fastest ice location begins to return to a more central position between the two sidewalls. Thickness drop ΔH increases proportionally with increasing promontory size L_p as seen in Figure 5 where a mean value of ΔH is calculated for each of the 10 T_s and $\dot{b}$ combinations for every particular L_p.

Our results reveal a similar correspondence between larger promontory sizes and higher downstream critical percentages. Considering a critical thickness of 75m, the mean downstream critical percentage is 28% for 10-60km promontories and 94% for 70-100km promontories.

Considering a critical thickness value of 50m, downstream critical percentages have a mean value of 1% for promontories 10-60km in size. For promontories 70-100km in size, the critical percentage rapidly increases, with a mean value of 34%.

5 Discussion

Figure 5c demonstrates a reduction in penetration length L as L_p increases. This result is physically sensible because the promontory partially blocks the channel and increasing L_p increases the perimeter of the channel and therefore the overall drag experienced by the sea glacier as it penetrates into the channel. This result suggests that the choice of rectangular channels in *Campbell et al.* [2014] represents an upper bound for sea-glacier penetration into channels, because the inclusion of promontories or islands will reduce sea-glacier penetration, consistent with the continental constriction experiments of *Tziperman et al.* [2012].

For our experiment, we test the model for sensitivity to promontory position by varying the promontory location from 0.1 L to 0.9 L; the thickness drop remains roughly constant (at ~340m) in the range of 0.1 L to 0.7 L and falls off sharply (from ~340 m to ~270 m) in the range of 0.7L to 0.9L. Despite the more significant thickness drop in the 0.1L - 0.7L range of positions, we chose a promontory location of 0.85 L in order to increase the likelihood of downstream ice thinning sufficiently to allow light to pass through.

Model outputs (i.e. h and L) varied among model runs even with similar inputs (i.e. T_s, $\dot{b}$ and L_p). The variance in model output is greater from adjusting T_s and $\dot{b}$ combinations than it is for adjusting values of L_p. The variance in model output by changing T_s and $\dot{b}$ combinations can be attributed to numerical noise internal to the model caused by differing meshed used in each

model iteration. In Figure 5 we use the mean values of the $\overline{H_U}$, $\overline{H_D}$, and *CP* to demonstrate the trend with increasing L_p, which is not obscured by the model variance.

The model's particularly large variance at L_p = 100 km can be understood through our model setup. Our model adjusts L_g until ice flux entering the channel through the upstream entrance (x = 0 km) balances ice flux leaving the channel through net sublimation. At the end of the channel a boundary condition is applied at $x = L_g$. In reality, the invading sea-glacier front would have a more complicated, likely parabolic shape, rather than the linear front specified in our model. This setup works well for channels of uniform width that are long and narrow, where the sea-glacier front is symmetric and best where the front is perpendicular to the sidewalls, but promontories near the front would cause the sea-glacier front to take a more complicated shape. When L_p = 100 km the size and location of the promontory are sufficient to alter the sea-glacier front from its assumed linear profile. It is here that numerical noise increases between runs of similar values of T_s and $\dot{b}$; hence the large variance for model runs where L_p = 100 km in Figure 5.

It is possible that an invading sea-glacier's surface would be higher than the surface of the promontory. We make the assumption that the promontory walls and the channel side walls are very steep and very high, which means the sea glacier cannot move onto the promontory. If the sea glacier were allowed to flow onto a shallow promontory, it might override the promontory, prohibiting an ice shadow. A grounded sea glacier flowing over a promontory would tend to slow because of the additional basal resistence. To model this effect would require a model capable of capturing basal resistance, which would be more complex than the model presented here.

6 Conclusions

We calculated the flow of floating ice around promontories for conditions suitable during a Snowball Earth event. We found the penetration of invading sea glaciers into channels is reduced with the introduction of a promontory. Ice flowing around a promontory is thinner downstream of the promontory relative to ice in a channel without a promontory; however, we were not able to conclusively demonstrate that ice downstream of the promontory would be thin enough allow for a refugium in the ice shadow. Modern examples and analogues can be found of both grounded and floating ice that thins as it flows around obstructions. For suitable conditions during the Snowball Earth events, sea-glacier ice could have thinned sufficiently on the downstream sides of large promontories in marine embayments to allow for photosynthesis.

7 Acknowledgements.

This research was supported by NSF grant ANT-11-42963.

8 Works Cited

Campbell, A. J., E. D. Waddington, and S. G. Warren (2011), Refugium for surface life on Snowball Earth in a nearly-enclosed sea? A first simple model for sea-glacier invasion, *Geophys. Res. Lett.*, *38*(19), 1–5, doi:10.1029/2011GL048846.

Campbell, A. J., E. D. Waddington, and S. G. Warren (2014), Refugium for surface life on Snowball Earth in a nearly enclosed sea? A numerical solution for sea-glacier invasion through a narrow strait, *J. Geophys. Res. Ocean.*, *119*(4), 2679–2690, doi:10.1002/2013JC009703.

Cuffey, K. M., and W. S. B. Paterson (2010), *The Physics of Glaciers*, 4th ed., Elsevier, Amsterdam.

Gelatt, T. S., C. S. Davis, I. Stirling, D. B. Siniff, C. Strobeck, and I. Delisle (2010), History and fate of a small isolated population of Weddell seals at White Island, Antarctica, *Conserv. Genet.*, *11*(3), 721–735, doi:10.1007/s10592-009-9856-6.

236 Glen, J. W. (1955), The Creep of Polycrystalline Ice, *Proc. R. Soc. A Math. Phys. Eng. Sci.*,
237 *228*(1175), 519–538, doi:10.1098/rspa.1955.0066.

238 Goodman, J. C. (2006), Through thick and thin: Marine and meteoric ice in a “Snowball Earth”
239 climate, *Geophys. Res. Lett.*, *33*(16), 2–5, doi:10.1029/2006GL026840.

240 Goodman, J. C., and R. T. Pierrehumbert (2003), Glacial flow of floating marine ice in “Snowball
241 Earth,” *J. Geophys. Res.*, *108*(3308), doi:10.1029/2002JC001471.

242 Knoll, A. (1992), The early evolution of eukaryotes: a geological perspective, *Science*,
243 *256*(5057), 622–627, doi:10.1126/science.1585174.

244 Li, D., and R. T. Pierrehumbert (2011), Sea glacier flow and dust transport on Snowball Earth,
245 *Geophys. Res. Lett.*, *38*(17), 1–4, doi:10.1029/2011GL048991.

246 Light, B., R. E. Brandt, and S. G. Warren (2009), Hydrohalite in cold sea ice: Laboratory
247 observations of single crystals, surface accumulations, and migration rates under a
248 temperature gradient, with application to “Snowball Earth,” *J. Geophys. Res.*, *114*(C7),
249 C07018, doi:10.1029/2008JC005211.

250 MacAyeal, D. R., V. Rommelaraere, P. Huybrechts, C. L. Hulbe, J. Determann, and C. Ritz
251 (1996), An ice-shelf model test based on the Ross Ice Shelf, Antarctica, *Ann. Glaciol.*, *23*,
252 46–51.

253 Macdonald, F. A, M. D. Schmitz, J. L. Crowley, C. F. Roots, D. S. Jones, A. C. Maloof, J. V
254 Strauss, P. A Cohen, D. T. Johnston, and D. P. Schrag (2010), Calibrating the
255 Cryogenian., *Science*, *327*(5970), 1241–3, doi:10.1126/science.1183325.

256 Morland, L. W. (1987), Unconfined ice-shelf flow, in *Dynamics of the West Antarctic Ice Sheet*,
257 edited by C. J. van der Veen and J. Oerlemans, pp. 99–116, Dordrecht, Kluwer Academic
258 Publishers.

259 Tziperman, E., D. S. Abbot, Y. Ashkenazy, H. Gildor, D. Pollard, C. G. Schoof, and D. P. Schrag
260 (2012), Continental constriction and oceanic ice-cover thickness in a Snowball-Earth
261 scenario, *J. Geophys. Res.*, *117*(C5), C05016, doi:10.1029/2011JC007730.

262 Warren, S. G., R. E. Brandt, T. C. Grenfell, and C. P. McKay (2002), Snowball Earth: Ice
263 thickness on the tropical ocean, *J. Geophys. Res.*, *107*(C10), 3167,
264 doi:10.1029/2001JC001123.

265

266

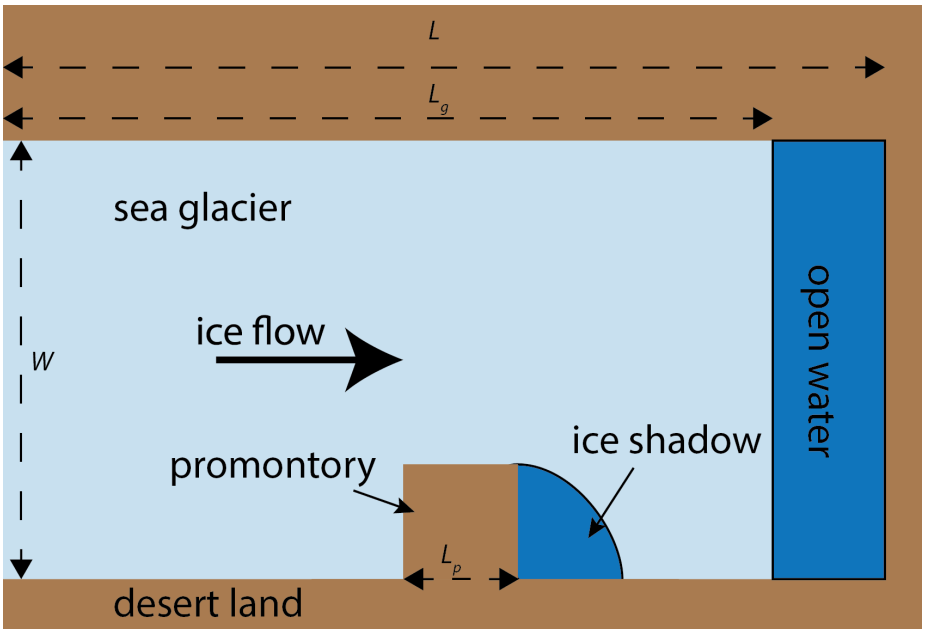

Figure 1. Cartoon illustration of ice shadow forming as sea glacier flows around a promontory in a channel.

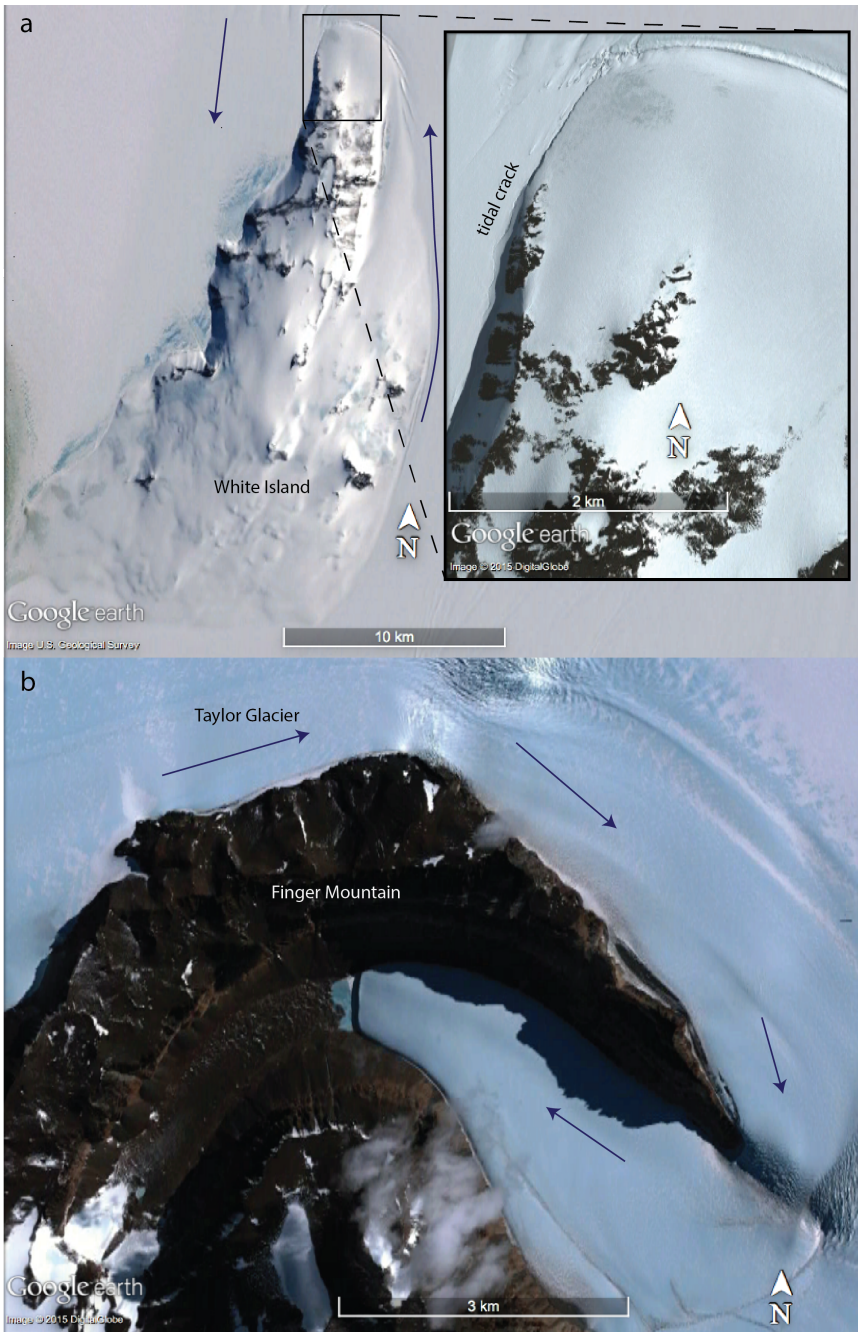
a
tidal crack
White Island
N
2 km
Google earth
Image © 2015 DigitalGlobe
N
Google earth
Image © U.S. Geological Survey
10 km
b
Taylor Glacier
Finger Mountain
Google earth
Image © 2015 DigitalGlobe
3 km
N

270

271 Figure 2. a) satellite image of Ross ice shelf flowing around White Island (78.1 °S, 167.4 °E) forming an ice shadow
272 on the northwest side of White Island where a tidal crack can form (inset). b) Taylor Glacier flowing around Finger
273 Mountain (77.8 °S, 161.3 °E) and incompletely penetrating Turnabout Valley. Arrows indicate the ice flow direction.

274

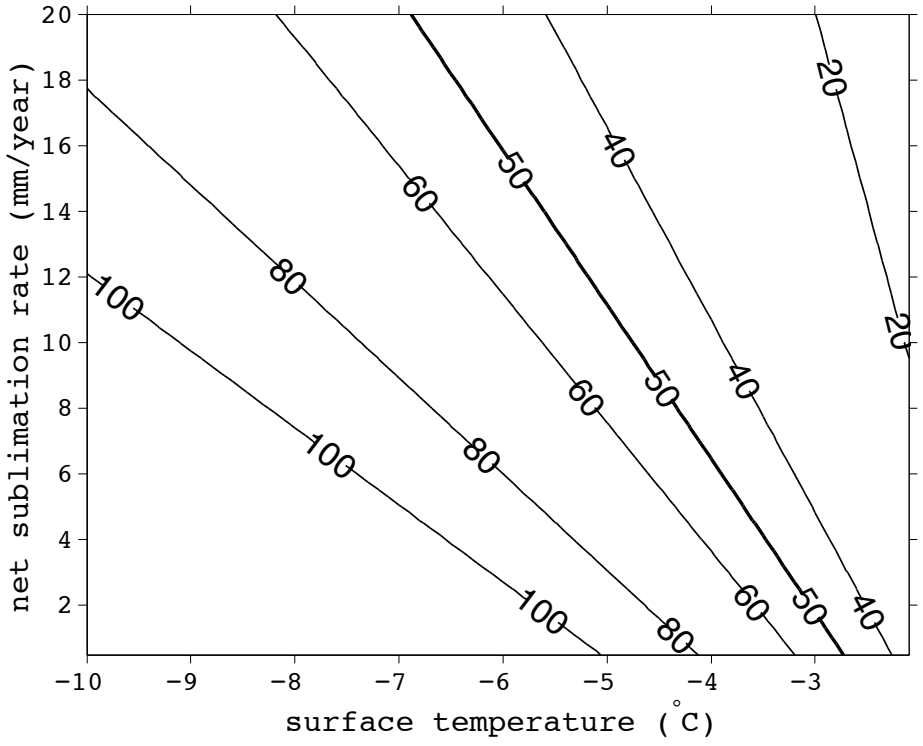

275

276 Figure 3. Ice thickness contours (in meters) for combinations of surface temperature and sublimation as predicted by
277 Equation 1.

278

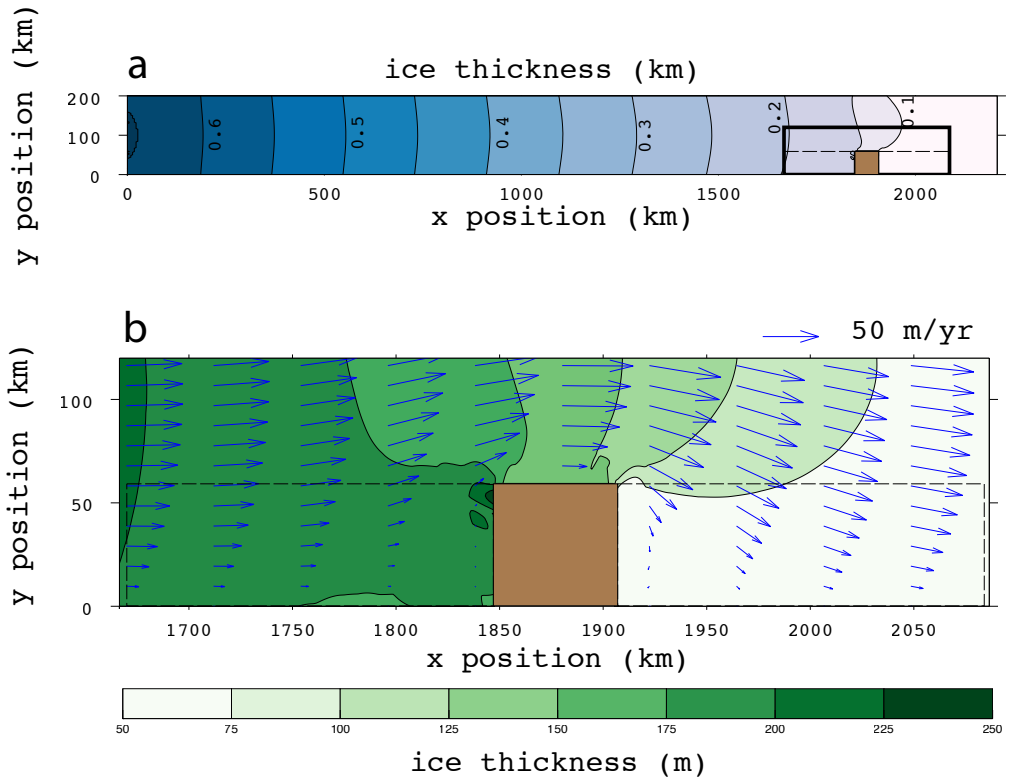

279

280

281 Figure 4. Results from a sample sea-glacier flow model where T_s = -5.33 °C, $\dot{b}$ = 12.70 mm/yr, L_p = 60 km. Arrows
282 indicate flow rate and direction; a reference arrow for 50 m/yr is shown. Contours show ice thickness. Dashed
283 rectangles indicate upstream (left) and downstream (right) regions where ice thickness is evaluated. (a) the entire
284 model domain, with a 50-m contour interval. (b) An enlarged section around the promontory, with a 25-m contour
285 interval.

286

287

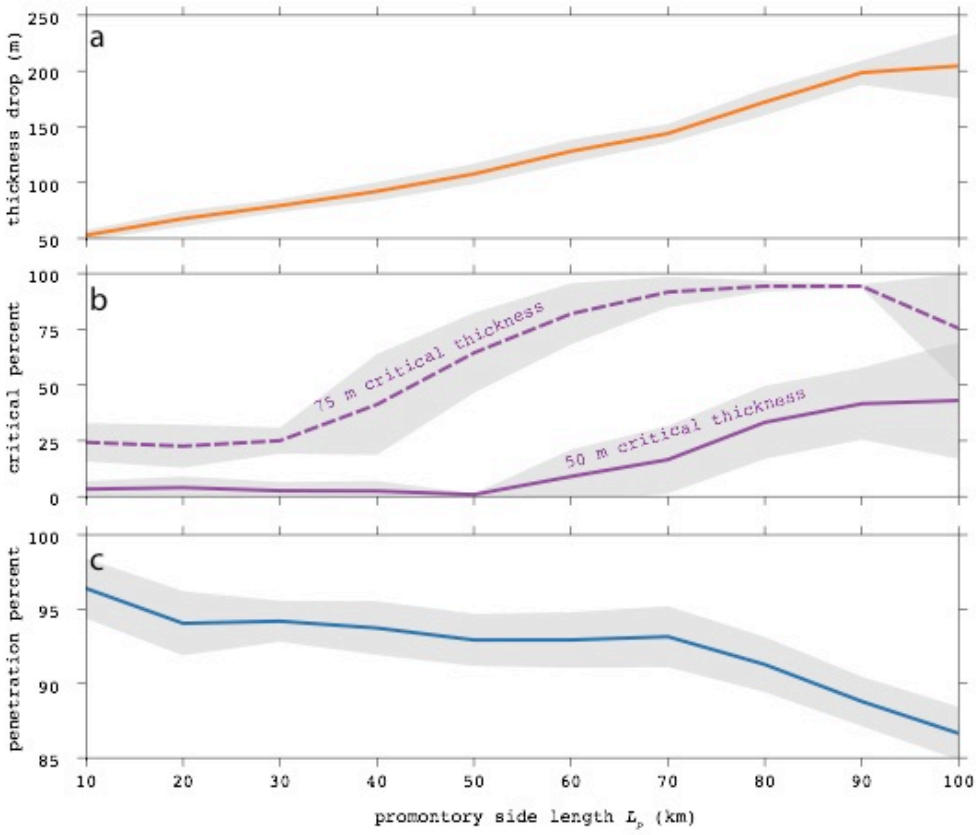

Figure 5. a) thickness drop ΔH b) critical percent for 50 m *CT* (solid) and 75 m *CT* (dashed), and c) penetration percent. For these experiments the channel width *W* is 200 km. Values are averaged over all T_s and $\dot{b}$ combinations for the particular promontory side length L_p. Gray outlines indicate the standard deviation.

50

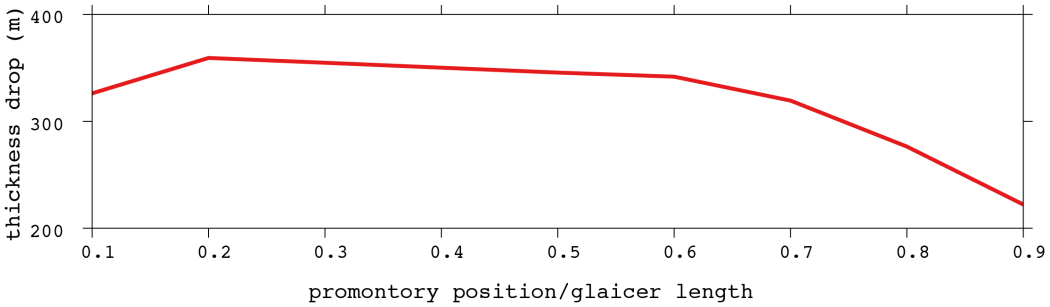

292

293 Figure 6. Thickness drop versus promontory position along sidewall. Promontory position is expressed here as a

294 fraction of the glacier's total penetration length. Sea-glacier terminus is to the right.

295

296

297

299 Table 1. Constants used in analysis.

Name	Symbol	Value	Units
geothermal flux	F_{geo}	0.1	W m^{-2}
acceleration of gravity	g	9.81	m s^{-2}
thermal conductivity of ice	k	2.5	W m^{-1} K^{-1}
latent heat of fusion of ice	L_i	3.3×10^5	J kg^{-1}
freezing temperature of sea water	T_f	-2	°C
ice density	ρ_i	917	kg m^{-3}

300

301

Chapter 6

CONCLUSIONS DRAWN FROM THIS WORK

Taken as a whole, this work represents a significant step forward in understanding where photosynthetic life may have survived during the Snowball Earth events. Without geologic evidence, it is impossible to prove that photosynthetic life survived in the restricted seaways I have described in this work. But this work does demonstrate that the photosynthetic life could survive on a planet with complete ice cover on the open ocean. No longer can we dismiss the Snowball Earth hypothesis on account of the evidence for survival of these organisms.

This work represents the first examination of refugia for photosynthetic life during the Snowball Earth events. In order for marine embayments to provide refugia for photosynthetic life, they must resist sea-glacier invasion. I have determined the climate and geometric conditions needed such that a marine embayment could restrict an invasion. The first paper of this work (Chapter 3) demonstrated that marine embayments could restrict such an invasion. The next two papers (Chapter 4 and 5) demonstrated that constraints on the geometry of the embayment would further diminish sea-glacier penetration.

Collectively, this work demonstrates that marine embayments are a viable option for the refuge of photosynthetic life during the Snowball Earth events. A snowball Earth event would be subject to a gradual warming before the Snowball state is destabilized. These works have demonstrated that marine embayment refugia's area would expand during the gradual warming of a Snowball Earth event, making them more robust refugia.

Chapter 7

THOUGHTS AND IDEAS FOR FURTHER RESEARCH

This dissertation has asked a question: could narrow marine embayments provide a refuge for photosynthetic life during the Snowball Earth events of the Neoproterozoic? The first paper of this work (Chapter 3) outlines four specific conditions needed for an inland sea to provide a refugium for photosynthetic organisms during Snowball Earth events:

> (1) the inland sea must not be fully penetrated by a sea glacier;
> (2) the climate on the inland sea must be such as to maintain it either ice-free or covered by an ice layer sufficiently thin to allow photosynthesis below the ice;
> (3) the depth of the sea at its entrance, and throughout its length, must be great enough that seawater is able to flow under the sea glacier to replenish water loss from the refugium by evaporation/sublimation, and
> (4) water circulation in the inland sea must be adequate to allow nutrients to be delivered to organisms living in the bay at the landward end.

Research described in Chapters 3, 4 and 5 demonstrates that condition (1) is viable. Here, I outline my present thoughts and ideas for addressing conditions (2) - (4) and other considerations such as land glaciers invading inland seas.

7.1 Climate of inland seas

An inland sea, free of sea-glacier invasion, could still freeze over with sea ice thick enough to prohibit the transmission of light, thus prohibiting the survival of photosynthetic life underneath the sea ice. Equilibrium sea ice thickness is determined by surface temperature, surface albedo, absorption within the ice, surface sublimation rate, and geothermal flux from below [Warren et al., 2002]. Warren et al. [2002] calculated ice thickness over the tropical ocean during conditions for a Snowball Earth event using a spectral radiation

model, coupled to a heat flow model, for surface temperatures around -30°C. They chose a temperature of -30°C because is it the warmest mean-annual surface temperature expected over the tropical ocean during the earliest portion of a Snowball Earth event. The earliest portion of a Snowball Earth event would have the thickest sea ice, having both the coldest temperatures and lowest net sublimation rates. Warren et al. [2002] concluded that sea ice would have been too thick to allow for photosynthesis below tropical ocean sea ice. Other studies [Pierrehumbert et al., 2011, Abbot and Pierrehumbert, 2010a, Abbot et al., 2012, 2013], have found mean-annual surface air temperatures over the ice-covered ocean to be consistent with -30°C used by Warren et al. [2002]; however Abbot and Pierrehumbert [2010a] found surface temperatures around 20°C warmer over equatorial continents than over the ice-cover ocean at the same latitude. The surface temperature over the land is warmer because the bare surface has a lower albedo than the ice-covered ocean.

Could inland seas be warmed by the surrounding low-albedo land masses? Inland seas in net-sublimation regions, could be surrounded by unglaciated desert land (see Section 7.3).

The effect of low albedo land on the mean-annual surface temperature over inland seas can be explored using a global circulation model (GCM). Many studies have used GCMs to study the climate conditions of the Neoproterozoic Snowball Earth events [Pierrehumbert et al., 2011]. Most climate studies of the Neoproterozoic have focused on situations without land, i.e. aquaplanets, while relatively few of these studies have considered the climate conditions of a planet that is covered in partially-bare land [Fiorella and Poulsen, 2013, Abbot and Pierrehumbert, 2010a, Voigt et al., 2011, Rodehacke et al., 2013]. Abbot and Pierrehumbert [2010a] found higher temperature and sublimation rate over bare-land regions when compared to sea glaciers at the same latitude. A GCM can be used to examine the climate of an inland sea in the context of a Snowball Earth event. An ice covered lake can be placed on a snow and ice free tropical continent in the GCM that is otherwise surrounded by an ice-covered ocean (Figure 7.1). The ice-covered lakes will vary in area and location (latitude and longitude). These tests can explore the local climate of inland water bodies in the context of the global climate.

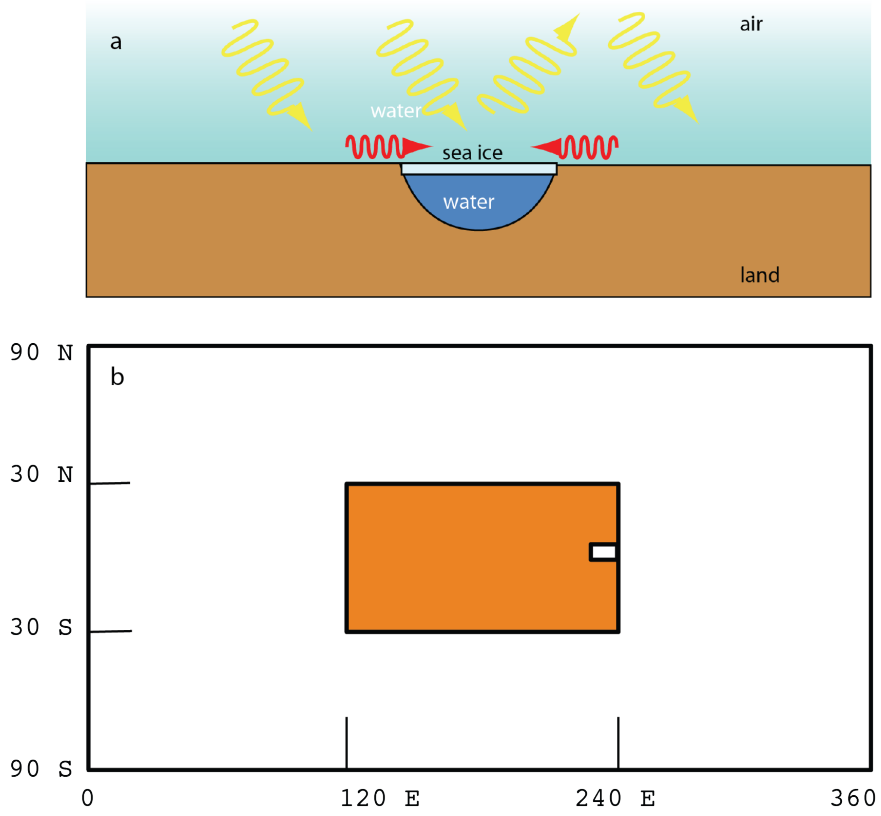

Figure 7.1: (a) Profile view cartoon of the proposed warming mechanism for a sea glacier invading an inland sea. Desert land will absorb relatively more light than the invading sea glacier (treated as "sea ice" in the GCM) because of their albedo contrast. (b) Map view cartoon of model setup, based on those used by Abbot and Pierrehumbert [2010a] and Fiorella and Poulsen [2013]. A rectangular continent, covered in bare desert is centered along the equator surrounded by ocean covered in sea ice.

7.2 Grounding of sea glaciers

This work has considering glaciers floating on water moving through restricted seaways, but not yet considering the effect of a sea glacier that becomes grounded. The Red Sea has been used as an analogue for restricted seaways in this work; however if a sea glacier were to penetrate into the Red Sea it would become grounded the shallow sill at the entrance. A model suitable for floating ice is simpler to solve and to understand. The complication

of allowing ice to become grounded adds a restrictive force to the penetrating sea glacier. I expect that any amount of sea-glacier grounding would reduce sea-glacier penetration into the channel. Therefore the models used in this work likely provide an upper limit for sea-glacier penetration.

The problem of sea-glacier grounding cannot be fully ignored. If a sea glacier completely grounds in the channel it may block ocean water from replenishing the refugium, effectively turning the refugium into a lake. In a desert region, that lake may eventually dry, destroying the refugium. There are several ways in which water may be replenished in the lake: seasonal surface melt may collect in the lake, basal melt may resupply the lake, the lake level may drop sufficiently to create a hydraulic gradient, driving water replenishment under the sea glacier, or ground water may flow into the lake.

If seasonal surface melt collects in the lake, the meltwater must come from a sufficient area such that the collected water can overcome the deficit of sublimation (or evaporation) over the lake. A sea-glacier surface would tend to slope downward toward the lake any melt on that surface would likely collect in the lake. As long as temperatures are warm enough around the lake to allow for seasonal melting, then it seems likely that the lake would have a means a replenishing itself and the lake could continue to be a refugium.

If the base of the sea glacier was at the melting point, melt water from the base could resupply the lake. To generate basal melt, heat production at the base of the sea glacier must exceed heat dissipation. Heat production is controlled by geothermal flux and friction. Heat dissipation is controlled by diffusion and advection. To completely solve this system a fully 3-D thermo-mechanical model must be used, however it may be possible to gain insight to this system with some simplifying assumptions.

If there is not enough melt to resupply the lake, the lake level would diminish over time. As the lake level lowers, the water would provide lower pressure on the sea-glacier front. Reduction of pressure at the sea-glacier front would allow the sea glacier to flow faster into the lake. As the sea glacier speeds up, it may become decoupled from its bed. As the sea glacier becomes decoupled from its bed, water which is overpressurized relative to the lake would move into the lake, replenishing the lake level. The increase in lake level would increase pressure at the sea-glacier front and may stabilize the sea-glacier advance.

Groundwater might resupply the lake. If the sea glacier were frozen to its bed, water in the bed material would also be frozen for some distance under the bed surface. Moving deeper under the bed surface, temperatures would eventually rise because of increasing temperature with depth inside the Earth. Therefore some depth below the sea glacier would allow for water to remain liquid. If a porous aquifer existed between the ocean and the lake, water from the ocean might resupply the lake, water flow being driven by a hydraulic pressure gradient. If we further conjecture that the sea glacier is invading into a spreading-center rift like the modern Red Sea, we could assume that the depth under the bed surface allowing for liquid water may be shallow because of an enhanced geothermal gradient. In addition, porous pillow basalts may form in the spreading-center rift allowing for water flow through the material. It may be possible to demonstrate this as a viable option by studying groundwater flow through existing aquifers in spreading centers. If extent, thickness, and hydraulic conductivity were known for typical spreading-center rifts, it would be possible to model the flow of groundwater under a sea glacier in a spreading-center.

In each of the cases described above, the lake that would be the refugium can adjust its size to balance water replenishment with losses. If the main source of loss is from sublimation or evaporation at the lake's upper surface, the lake could lower its volume to reduce losses from its upper surface area. However, each of the potential replenishment ideas explored here is either unaffected or increases with decreasing lake volume. Therefore it is possible that a smaller lake may balance water losses with gains. Smaller lakes have the drawback that they provide less habitat for surviving organisms and may be more susceptible to destruction. Even if a method of lake destruction is reversible, the organisms may die off and be unable to repopulate the refugium.

7.3 Land glaciers

Inland seas could not have been refugia for photosynthetic eukaryotes if they were overrun by land-based glaciation. The degree of land glaciation during the Snowball Earth Events of the Neoproterozoic is unknown. Dropstones and diamictites deposited at near-equatorial paleolatitudes [Hoffman et al., 1998] have led many to assume that land-based glaciers covered all, or most land during the Sturtian and Marinoan glaciations [Hoffman and Schrag,

2002]. This assumption continues to be the prevalent in recent thinking [Creveling and Mitrovica, 2014]. However, climate models reliably demonstrate a zone of net sublimation centered along the equator [Abbot et al., 2013], the physical mechanism for this is explained in Pierrehumbert et al. [2011]. The zone of net sublimation typically extends from around 10°N to 10°S in climate models for an aquaplanet Snowball Earth. The presence of bare land acts to enhance sublimation [Abbot and Pierrehumbert, 2010a] and bare continents might extend outside that zone and still experience net sublimation (Figure 7.2). This leads to the conclusion that a flat continent, entirely contained within that zone, could not support land-based glaciation. This continent would be bare if sea glaciers are unable to penetrate the continent.

A flat continent, entirely contained within a zone of net sublimation, could not support land-based glaciation. However, no continent is perfectly flat and continents might extend outside of the zone of net sublimation. I propose two questions: Would mountains act to seed glaciation on otherwise flat continents in the net sublimation zone? Could continents, partially outside the zone of net sublimation, still contain bare land? If so, what are the bounds to this problem?

7.3.1 Mountains seeding continental glaciation

Would mountains act to seed glaciation on otherwise flat continents in the net sublimation zone? Rodehacke et al. [2013] used an ice sheet model, coupled to and ocean-atmosphere GCM to bound the size of an open-water sea-way still allowing for land glaciation, for conditions suitable during a Neoproterozoic Snowball Earth event. They showed that mountains are able to seed continental glaciation [Rodehacke et al., 2013, Figure 1]; however they have difficulty penetrating into warmer, low-latitude regions. There are two factors that may act to overestimate mountain-seeded glaciation in Rodehacke et al. [2013]. Firstly, they use a Gaussian distribution for mountain region hyposometry; however present-day Earth's continental hypsometry more closely resembles a decaying exponential [Eakins and Sharman, 2012]. Their choice of hyposometry would exaggerate the accumulation zone of mountain glaciers and therefore increase the size of land glaciation. Secondly, their model

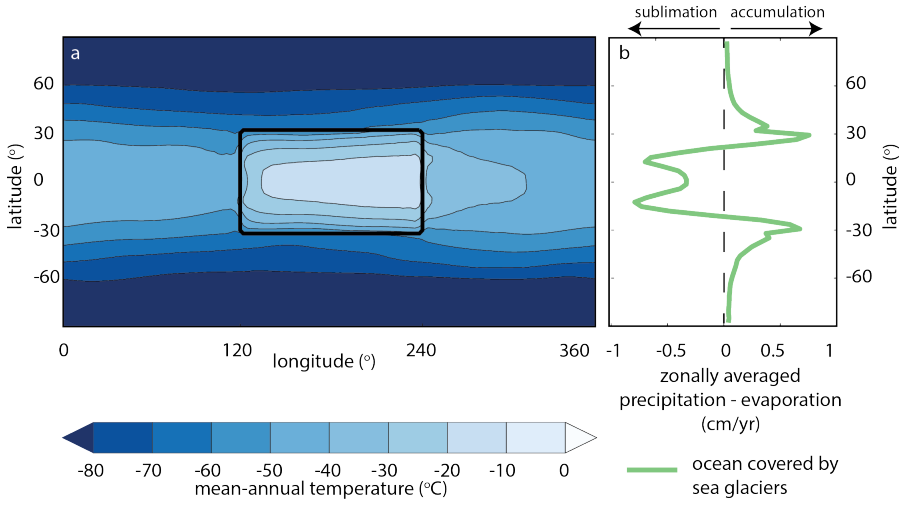

Figure 7.2: (a) mean annual temperature for a rectangular continent, covered in bare, desert is centered along the equator surrounded by ocean covered in sea ice from a Snowball Earth Climate model. (b) zonally-average accumulation minus sublimation rates for that same model. Figure modified from Abbot and Pierrehumbert [2010a]

exclusively used a positive-degree-day ablation scheme for ablating land ice [Ziemen, 2013]. The positive-degree-day ablation scheme is incapable of ablating ice through sublimation at sub-freezing temperatures. Ablation through sublimation is the main source of ablation for many modern-day glaciers, particularly glaciers in the McMurdo Dry Valleys and the Allan Hills of Antarctica [Dadic et al., 2013]. These glaciers are thought to be the best modern analogues for glaciers during Snowball Earth events because they ablate primarily through sublimation.

An over-estimation of the accumulation zone and neglecting of sublimation as a form of ablation led [Rodehacke et al., 2013] to overestimate the extent of glaciation seeding by mountain glaciation. [Rodehacke et al., 2013] determined that mountain glaciers have difficulty penetrating into warmer, low-latitude regions in their models. If a realistic hypsometry and ablation through sublimation were also included in their model, mountain glaciers would have even further difficulty penetrating into warmer, low-latitude regions.

7.3.2 Continents outside the sublimation zone

Could continents, partially outside the zone of net sublimation, still contain bare land? If so, what are the bounds to this problem? For a continent to be completely covered in land glaciers, the area-integrated accumulation must exceed area-integrated sublimation. Land glaciers flow from accumulation regions to ablation regions. How extensively glaciated would continents have been during the Snowball Earth events? A simple first approach might be to take a continental land distribution such as the one used in Creveling and Mitrovica [2014], apply a simple Shallow Ice Approximation ice flow model forced with a zonally averaged surface mass balance from Pierrehumbert et al. [2011]. Pierrehumbert et al. [2011] has zonally averaged surface mass balance for aquaplanets which have smaller regions of net sublimation than Abbot and Pierrehumbert [2010a] which has a bare land continent centered at the equator. If an ice flow model forced with aquaplanet conditions was capable of generating bare land without the benefit of enhanced sublimation, it is difficult to see how bare land could not persist in the Snowball Earth climate state.

7.4 Nutrient supply

For organisms to survive in a refugium they must receive nutrients. This is possible in a close inland sea if organism remnants can be recycled. For this to happen the sea would need to experience upwelling and not be completely stratified. If the sea were open and received melt water input, it is possible that melt water would contain nutrients capable of sustaining the refugium. In addition, meltwater that runs off the continent seasonally may have provided these nutrients in the form of minerals.

BIBLIOGRAPHY

Dorian S. Abbot and Raymond T. Pierrehumbert. Mudball: Surface dust and Snowball Earth deglaciation. *Journal of Geophysical Research*, 115(D3):1–40, February 2010a. ISSN 0148-0227. doi: 10.1029/2009JD012007. URL http://www.agu.org/pubs/crossref/2010/2009JD012007.shtml.

Dorian S. Abbot and Raymond T. Pierrehumbert. Mudball: Surface dust and Snowball Earth deglaciation. *Journal of Geophysical Research*, 115(D3):1–11, February 2010b. ISSN 0148-0227. doi: 10.1029/2009JD012007. URL http://www.agu.org/pubs/crossref/2010/2009JD012007.shtml.

Dorian S. Abbot, Aiko Voigt, and Daniel Koll. The Jormungand global climate state and implications for Neoproterozoic glaciations. *Journal of Geophysical Research*, 116 (D18):1–14, September 2011. ISSN 0148-0227. doi: 10.1029/2011JD015927. URL http://www.agu.org/pubs/crossref/2011/2011JD015927.shtml.

Dorian S. Abbot, Aiko Voigt, Mark Branson, Raymond T. Pierrehumbert, David Pollard, Guillaume Le Hir, and Daniel D. B. Koll. Clouds and Snowball Earth deglaciation. *Geophysical Research Letters*, 39(20):2–5, October 2012. ISSN 0094-8276. doi: 10.1029/2012GL052861. URL http://www.agu.org/pubs/crossref/2012/2012GL052861.shtml.

Dorian S. Abbot, Aiko Voigt, Dawei Li, Guillaume Le Hir, Raymond T. Pierrehumbert, Mark Branson, David Pollard, and Daniel D. B. Koll. Robust elements of Snowball Earth atmospheric circulation and oases for life. *Journal of Geophysical Research Atmospheres*, 118, 2013. doi: 10.1002/jgrd.50540. URL http://onlinelibrary.wiley.com/wol1/doi/10.1002/jgrd.50540/full.

M. I. Budyko. The effect of solar radiation variations on the climate of the Earth. *Tellus*, 21(5):611–619, October 1969. ISSN 00402826. doi: 10.1111/j.2153-3490.1969.tb00466.x. URL http://tellusa.net/index.php/tellusa/article/view/10109.

Adam J. Campbell, Edwin D. Waddington, and Stephen G. Warren. Refugium for surface life on Snowball Earth in a nearly-enclosed sea? A first simple model for sea-glacier invasion. *Geophysical Research Letters*, 38(19):1–5, October 2011. ISSN 0094-8276. doi: 10.1029/2011GL048846. URL http://www.agu.org/pubs/crossref/2011/2011GL048846.shtml.

Adam J. Campbell, Edwin D. Waddington, and Stephen G. Warren. Refugium for surface life on Snowball Earth in a nearly enclosed sea? A numerical solution for sea-glacier invasion through a narrow strait. *Journal of Geophysical Research: Oceans*, 119 (4):2679–2690, 2014. doi: 10.1002/2013JC009703.

Jessica R. Creveling and Jerry X. Mitrovica. The sea-level fingerprint of a Snowball Earth deglaciation. *Earth and Planetary Science Letters*, 399:74–85, August 2014. ISSN 0012821X. doi: 10.1016/j.epsl.2014.04.029. URL `http://linkinghub.elsevier.com/retrieve/pii/S0012821X14002696`.

Ruzica Dadic, Peter C. Mullen, Martin Schneebeli, Richard E. Brandt, and Stephen G. Warren. Effects of bubbles, cracks, and volcanic tephra on the spectral albedo of bare ice near the Transantarctic Mountains: Implications for sea glaciers on Snowball Earth. *Journal of Geophysical Research: Earth Surface*, 118(3):1658–1676, 2013. ISSN 21699011. doi: 10.1002/jgrf.20098.

B. W. Eakins and G. F Sharman. Hypsographic Curve of Earth's Surface from ETOPO1. Technical report, NOAA National Geophysical Data Center, Boulder, CO, 2012.

Ryan C. Ewing, Ian Eisenman, Michael P. Lamb, Laura Poppick, Adam C. Maloof, and Woodward W. Fischer. New constraints on equatorial temperatures during a Late Neoproterozoic snowball Earth glaciation. *Earth and Planetary Science Letters*, 406: 110–122, November 2014. ISSN 0012821X. doi: 10.1016/j.epsl.2014.09.017. URL `http://linkinghub.elsevier.com/retrieve/pii/S0012821X1400572X`.

Richard P. Fiorella and Christopher J. Poulsen. Dehumidification over Tropical Continents Reduces Climate Sensitivity and Inhibits Snowball Earth Initiation. *Journal of Climate*, 26(23):9677–9695, December 2013. ISSN 0894-8755. doi: 10.1175/JCLI-D-12-00820.1. URL `http://journals.ametsoc.org/doi/abs/10.1175/JCLI-D-12-00820.1`.

Paul F. Hoffman and Daniel P Schrag. Snowball Earth. *Scientific American*, 282(1): 68–75, 2000.

Paul F. Hoffman and Daniel P Schrag. The snowball Earth hypothesis : testing the limits of global change. *Terra Nova*, 14(3):129–155, 2002.

Paul F. Hoffman, Alan J. Kaufman, Galen P. Halverson, and Daniel P. Schrag. A Neoproterozoic Snowball Earth. *Science*, 281(5381): 1342–1346, August 1998. doi: 10.1126/science.281.5381.1342. URL `http://www.sciencemag.org/cgi/doi/10.1126/science.281.5381.1342`.

W. T. Hyde, Thomas J. Crowley, S. K. Baum, and W. R. Peltier. Neoproterozoic 'snowball Earth' simulations with a coupled climate/ice-sheet model. *Nature*, 405(6785):425–9, May 2000. ISSN 0028-0836. doi: 10.1038/35013005. URL http://www.ncbi.nlm.nih.gov/pubmed/10839531.

J. L. Kirschvink. Late Proterozoic Low-Latitude Global Glaciation: the Snowball Earth. In J.W. Schopf and C. Klein, editors, *The Proterozoic Biosphere*, chapter 2.3, pages 51–52. Cambridge University Press, New York, 1992.

A. Knoll. The early evolution of eukaryotes: a geological perspective. *Science*, 256 (5057):622–627, May 1992. ISSN 0036-8075. doi: 10.1126/science.1585174. URL http://www.sciencemag.org/cgi/content/abstract/256/5057/622.

Guillaume Le Hir, Gilles Ramstein, Yannick Donnadieu, and Yves Goddéris. Scenario for the evolution of atmospheric pCO2 during a snowball Earth. *Geology*, 36(1):47, 2008. ISSN 0091-7613. doi: 10.1130/G24124A.1. URL http://geology.gsapubs.org/cgi/doi/10.1130/G24124A.1.

Guillaume Le Hir, Yannick Donnadieu, Gerhard Krinner, and Gilles Ramstein. Toward the snowball earth deglaciation.... *Climate Dynamics*, 35(2-3):285–297, January 2010. ISSN 0930-7575. doi: 10.1007/s00382-010-0748-8. URL http://link.springer.com/10.1007/s00382-010-0748-8.

Dawei Li and Raymond T. Pierrehumbert. Sea glacier flow and dust transport on Snowball Earth. *Geophysical Research Letters*, 38(17):n/a–n/a, September 2011. ISSN 00948276. doi: 10.1029/2011GL048991. URL http://doi.wiley.com/10.1029/2011GL048991.

Yonggang Liu and W. Richard Peltier. A carbon cycle coupled climate model of Neoproterozoic glaciation: Influence of continental configuration on the formation of a soft snowball. *Journal of Geophysical Research*, 115(D17): D17111, September 2010. ISSN 0148-0227. doi: 10.1029/2009JD013082. URL http://doi.wiley.com/10.1029/2009JD013082.

Gordon D Love, Emmanuelle Grosjean, Charlotte Stalvies, David a Fike, John P Grotzinger, Alexander S Bradley, Amy E Kelly, Maya Bhatia, William Meredith, Colin E Snape, Samuel a Bowring, Daniel J Condon, and Roger E Summons. Fossil steroids record the appearance of Demospongiae during the Cryogenian period. *Nature*, 457(7230):718–721, 2009. ISSN 0028-0836. doi: 10.1038/nature07673. URL http://dx.doi.org/10.1038/nature07673.

Francis a Macdonald, Mark D Schmitz, James L Crowley, Charles F Roots, David S Jones, Adam C Maloof, Justin V Strauss, Phoebe a Cohen, David T Johnston, and Daniel P Schrag. Calibrating the Cryogenian. *Science (New York, N.Y.)*, 327

(5970):1241–3, March 2010. ISSN 1095-9203. doi: 10.1126/science.1183325. URL http://www.ncbi.nlm.nih.gov/pubmed/20203045.

Adam C. Maloof, James B. Kellogg, and Alison M. Anders. Neoproterozoic sand wedges: Crack formation in frozen soils under diurnal forcing during a snowball Earth. *Earth and Planetary Science Letters*, 204(1-2):1–15, 2002. ISSN 0012821X. doi: 10.1016/S0012-821X(02)00960-3.

Adam C. Maloof, Catherine V. Rose, Robert Beach, Bradley M. Samuels, Claire C. Calmet, Douglas H. Erwin, Gerald R. Poirier, Nan Yao, and Frederik J. Simons. Remains of pre-Marinoan sponges ? Dispersed in the west limestones from South Australia. *Nature Geoscience*, 3(9), 2010. doi: 10.1038/NGEO934.

Daniel B Mills, Lewis M Ward, CarriAyne Jones, Brittany Sweeten, Michael Forth, Alexander H Treusch, and Donald E Canfield. Oxygen requirements of the earliest animals. *Proceedings of the National Academy of Sciences*, 111 (11):4168–4172, 2014. ISSN 1091-6490. doi: 10.1073/pnas.1400547111. URL http://www.pnas.org/content/111/11/4168.abstract.

J. F. Nye. The flow of a glacier in a channel of rectangular, elliptical or parabolic cross-section. *Journal of Glaciology*, 5(41):661–690, 1965.

Alison N Olcott, Alex L Sessions, Frank a Corsetti, Alan J Kaufman, and Tolentino Flavio de Oliviera. Biomarker evidence for photosynthesis during neoproterozoic glaciation. *Science (New York, N.Y.)*, 310(5747):471–474, 2005a. ISSN 0036-8075. doi: 10.1126/science.1115769.

Alison N Olcott, Alex L Sessions, Frank A Corsetti, Alan J Kaufman, and Tolentino Flavio de Oliviera. Biomarker evidence for photosynthesis during neoproterozoic glaciation. *Science*, 310(5747):471–4, October 2005b. ISSN 1095-9203. doi: 10.1126/science.1115769. URL http://www.ncbi.nlm.nih.gov/pubmed/16195425.

Raymond T. Pierrehumbert, Dorian S. Abbot, Aiko Voigt, and Daniel D. B. Koll. Climate of the Neoproterozoic. *Annual Review of Earth and Planetary Sciences*, 39(1): 417–460, May 2011. ISSN 0084-6597. doi: 10.1146/annurev-earth-040809-152447. URL http://www.annualreviews.org/doi/abs/10.1146/annurev-earth-040809-152447.

David Pollard and James F. Kasting. Snowball Earth: A thin-ice solution with flowing sea glaciers. *Journal of Geophysical Research*, 110 (C07010), 2005. ISSN 0148-0227. doi: 10.1029/2004JC002525. URL http://www.agu.org/pubs/crossref/2005/2004JC002525.shtml.

L. A. Riedman, S. M. Porter, G. P. Halverson, M. T. Hurtgen, and C. K. Junium. Organic-walled microfossil assemblages from glacial and interglacial Neoproterozoic units of Australia and Svalbard. *Geology*, 42(11):

1011–1014, October 2014. ISSN 0091-7613. doi: 10.1130/G35901.1. URL http://geology.gsapubs.org/cgi/doi/10.1130/G35901.1.

Christian B. Rodehacke, Aiko Voigt, Florian Ziemen, and Dorian S. Abbot. An open ocean region in Neoproterozoic glaciations would have to be narrow to allow equatorial ice sheets. *Geophysical Research Letters*, 40(20):5503–5507, October 2013. ISSN 00948276. doi: 10.1002/2013GL057582. URL http://doi.wiley.com/10.1002/2013GL057582.

Brian E J Rose. Stable Waterbelt climates controlled by tropical ocean heat transport : A nonlinear coupled climate mechanism of relevance to Snowball Earth. *Journal of Geophysical Research: Atmospheres*, pages 1404–1423, 2015. doi: 10.1002/2014JD022659.Received.

William D. Sellers. A Global Climatic Model Based on the Energy Balance of the Earth-Atmosphere System. *Journal of Applied Meteorology*, 8(3):392–400, June 1969. ISSN 0021-8952.

Eli Tziperman, Dorian S. Abbot, Yosef Ashkenazy, Hezi Gildor, David Pollard, Christian G. Schoof, and Daniel P. Schrag. Continental constriction and oceanic ice-cover thickness in a Snowball-Earth scenario. *Journal of Geophysical Research*, 117(C5):C05016, May 2012. ISSN 0148-0227. doi: 10.1029/2011JC007730. URL http://doi.wiley.com/10.1029/2011JC007730.

Aiko Voigt, Dorian S. Abbot, Raymond T. Pierrehumbert, and J. Marotzke. Initiation of a Marinoan Snowball Earth in a state-of-the-art atmosphere-ocean general circulation model. *Climate of the Past*, 7(1):249–263, March 2011. ISSN 1814-9332. doi: 10.5194/cp-7-249-2011. URL http://www.clim-past.net/7/249/2011/.

Stephen G. Warren, Richard E. Brandt, Thomas C. Grenfell, and Christopher P. McKay. Snowball Earth: Ice thickness on the tropical ocean. *Journal of Geophysical Research*, 107(C10):3167, 2002. ISSN 0148-0227. doi: 10.1029/2001JC001123. URL http://www.agu.org/pubs/crossref/2002/2001JC001123.shtml.

Florian Andreas Ziemen. Glacial Climate Variability. *Berichte zur Erdsystemforschung*, 139:140pp, 2013. ISSN 1614-1199.